Technical Note

1975-3

Some Characteristics of a Communication Satellite Multiple-Beam Antenna

L. J. Ricardi

A. J. Simmons

A. R. Dion

L. K. DeSize

B. M. Potts

28 January 1975

Prepared for the Defense Communications Agency
under Electronic Systems Division Contract F19628-73-C-0002 by

Lincoln Laboratory

MASSACHUSETTS INSTITUTE OF TECHNOLOGY

LEXINGTON, MASSACHUSETTS

The work reported in this document was performed at Lincoln Laboratory, a center for research operated by Massachusetts Institute of Technology, for the Military Satellite Office of the Defense Communications Agency under Air Force Contract F19628-73-C-0002.

This technical report has been reviewed and is approved for publication.

FOR THE COMMANDER

Eugene C. Raabe

Eugene C. Raabe, Lt. Col., USAF
Chief, ESD Lincoln Laboratory Project Office

MASSACHUSETTS INSTITUTE OF TECHNOLOGY

LINCOLN LABORATORY

SOME CHARACTERISTICS OF A COMMUNICATION SATELLITE MULTIPLE-BEAM ANTENNA

L. J. RICARDI
A. J. SIMMONS
A. R. DION
L. K. DeSIZE
B. M. POTTS
Group 61

TECHNICAL NOTE 1975-3

28 JANUARY 1975

LEXINGTON MASSACHUSETTS

ABSTRACT

A deployed satellite communication system can become obsolescent due to changing equipment, facilities or requirements of the users. This obsolescence is often due to the lack of flexibility of the satellite's antennas. A multiple-beam antenna has inherent characteristics which allow its radiation pattern to be varied with electronic ease and at an electronic rate. The flexibility of such an antenna should reduce the rate of obsolescence of Defense Satellite Communication System satellites. This note describes a multiple-beam antenna, consisting of a waveguide lens antenna system excited by a variable beam-forming network capable of producing a wide range of radiation patterns. These patterns vary from a narrow high-gain beam, equivalent to that of a steerable paraboloid, to the earth-coverage pattern of a wide-coverage communication satellite. The latter can be modified to suppress interfering signals by radiation pattern shaping. An accurate method of analysis, supported by experimental data, is used to derive the minimum directive gain of the antenna system over its field-of-view. Two methods of producing earth-coverage patterns with prescribed minima and a flexible beam-forming network capable of forming these radiation patterns are discussed.

SOME CHARACTERISTICS OF A COMMUNICATION SATELLITE MULTIPLE-BEAM ANTENNA

I. INTRODUCTION

A previous paper[1] describing the use of a multiple-beam antenna in a communication satellite introduced the subject and presented some experimental results and analytic techniques. A recent need for more knowledge about this multiple-beam antenna provided motivation to determine more of its fundamental characteristics. Toward this end, a study, sponsored by the Military Satellite Office of the Defense Communication Agency, of the beam scanning characteristics, maximum achievable directive gain, and the network for beam-forming and pattern shaping was initiated. This note presents some initial analytic and experimental results from this study. The first section describes the antenna system and method of analysis. This is followed by a description of the beam scanning and maximum directive gain characteristics. The next section on producing an earth-coverage radiation pattern with prescribed minima, which is of interest for reducing interference on reception, demonstrates the true versatility of a multiple-beam antenna. A section comparing calculated and experimental data and a discussion of the beam-forming network completes this note.

II. A VARIABLE-COVERAGE LENS ANTENNA

There are many antenna configurations that could be suitable as the radiating component of a multiple-beam antenna system. We have chosen a particular configuration which seems to us to be a reasonable one for satellite communications. This antenna, upon which much of the calculated and

all of the measured data are based, is shown in Fig. 1. The design and performance of this antenna are not optimum for a synchronous satellite; rather it serves as a test bed to ascertain the accuracy of the analytical method presented. It consists of a waveguide lens $\approx$ 30 inches in diameter with focal length = 30 inches and contains approximately 700 titanium waveguides with a 1.0" x 1.0" square cross section and a .005" wall thickness. This assembly of waveguides (not including the outer support ring or the booms) weighs but 7 lbs. It is illuminated by an array of 19 conical horns arranged in an equilateral triangular grid. The circular apertures of these horns lie in a plane perpendicular to the focal axis of the lens and $\approx$ 30" from the vertex of the lens. The inner surface of the lens is spherical with a radius of 30". The length of the individual waveguides in the lens is adjusted to produce the phase advance necessary to convert the incident "spherical" wave (i.e., considering the antenna as transmitting signals) into a "plane" wave. The length of those waveguides which introduce a phase advance greater than 360° is reduced so as to decrease the phase advance by $n \times 360°$ where n = 1 or 2. This results in a "stepped" or "zoned" lens as characterized by the outer surface of the lens. The details of this design are presented elsewhere[1] and summarized here only for completeness.

The conical horns have circular apertures with diameter, d, equal to the spacing, s, between adjacent horns. Since s is an important parameter in obtaining a desired performance, specific values will be given later. The horns are excited by a loop so that each feed radiates a linearly polarized signal. The measured data reported here were obtained by exciting the

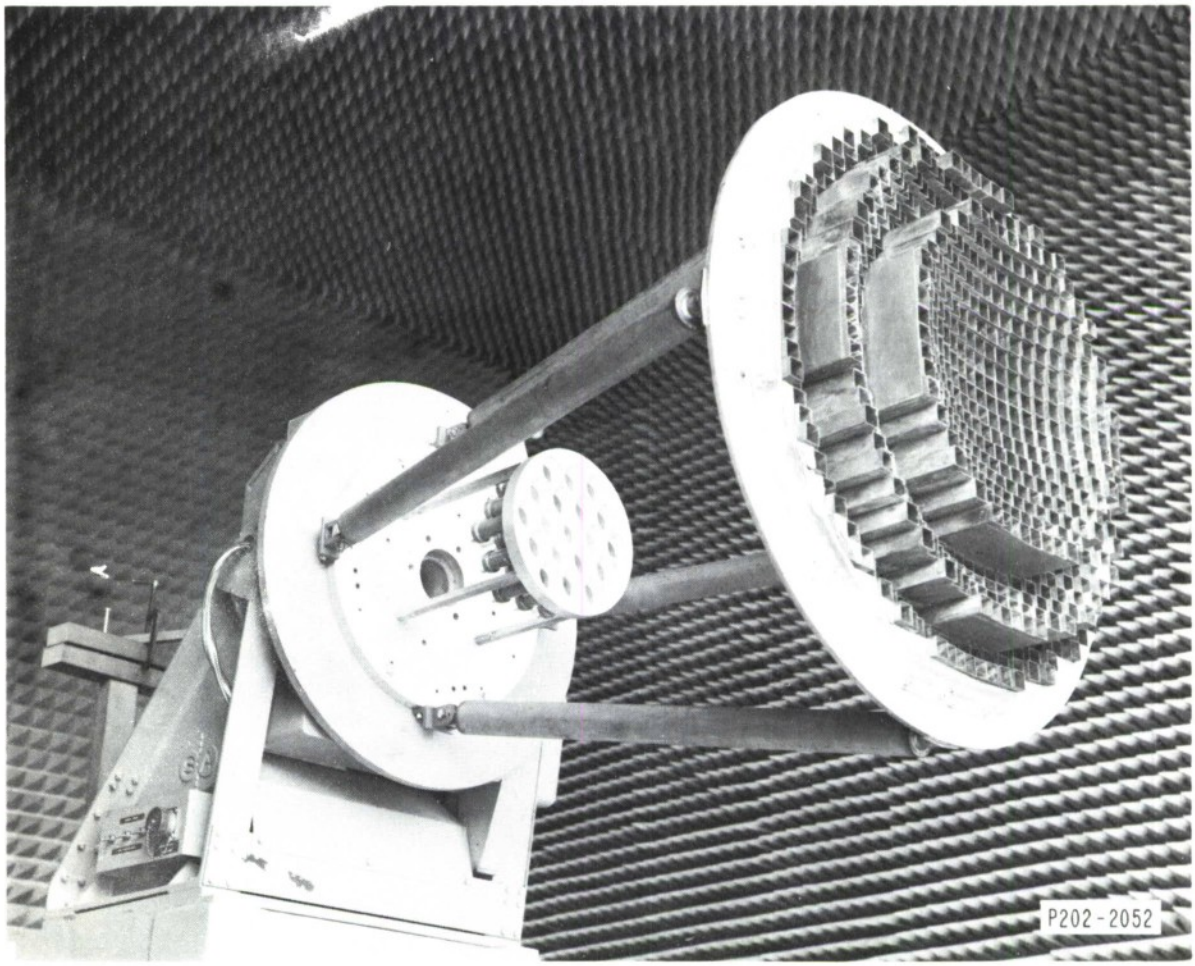

Fig. 1. LES-7 multiple beam lens antenna.

feed horns through a lossy 19-to-1 power divider. However, the beam-forming network described in the next section will eventually be used with the antenna system (Fig. 1) to demonstrate the versatility of a multiple-beam antenna system.

III. BEAM-FORMING NETWORK

There are many networks by which the multiple feeds can be connected to a transmitter to obtain variable radiation patterns. This network, which is appropriately called a beam-forming network (BFN), largely determines the versatility of the antenna system. The BFN described in this note is a corporate feed network made of continuously variable, as opposed to fixed, power dividing junctions. (Switches are not considered variable power dividers since they provide a finite fixed set of power distributions). A schematic representation of the BFN is shown in Fig. 2. With this network, any desired power distribution may be obtained at the output ports. With such a network one is not limited to only 19 pencil beams, as would be the case if energy were merely switched from one of the 19 horns to another, but, by properly dividing the power among several adjacent horns, pencil beams may be formed in any desired direction within the field-of-view.

The variable power dividing junctions (VPD's) consist of a 3-dB hybrid coupler, two non-reciprocal latching ferrite phase shifters and a modified magic "tee" with a matched waveguide load on its "difference" port. Let us first discuss these components separately and then as a complete assembly.

The 3-dB hybrid coupler is shown in Fig. 3. Understanding its properties is the key to understanding the VPD. Basically, it is made of two

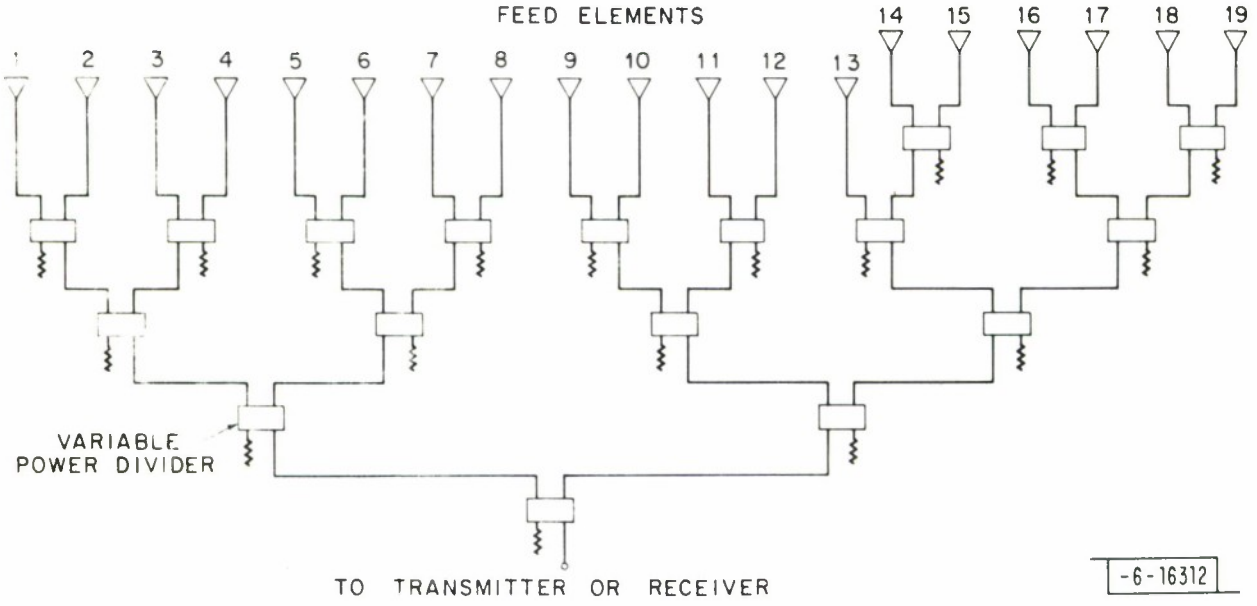

Fig. 2. Beam-forming network, schematic.

18-6-16313

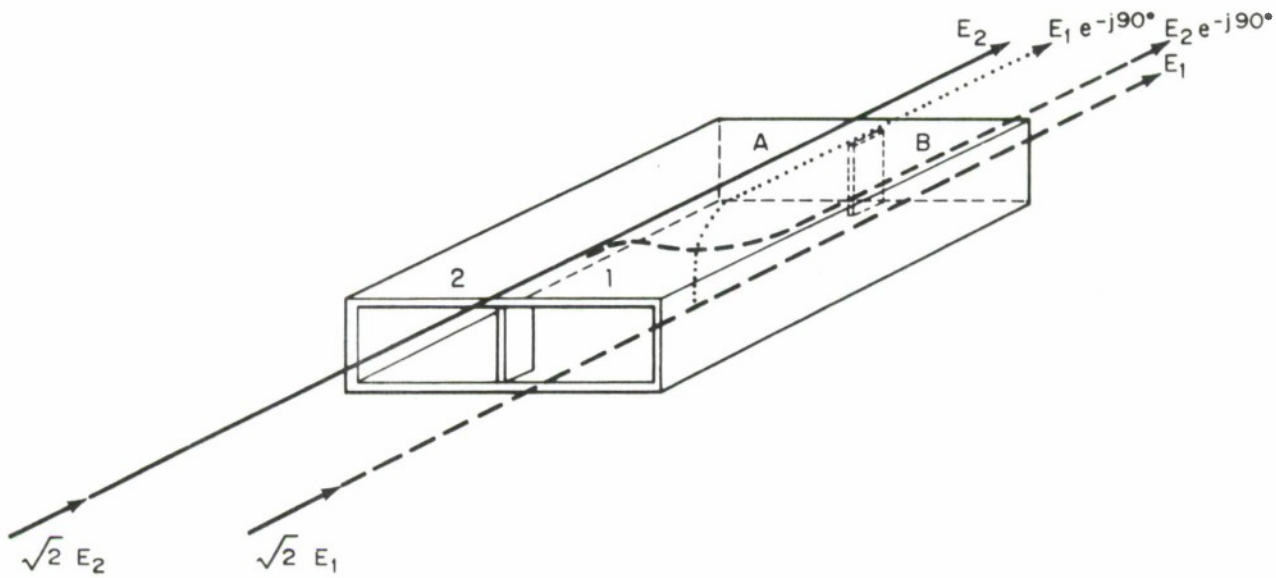

Fig. 3. 3 dB hybrid coupler.

standard rectangular waveguides which have a common "narrow", or side, wall. The energy traveling in one guide is coupled to the other by removing the common wall between guides for an appropriate length along the guide axis. Small sections of the common wall are shown (Fig. 3) at the input and output ends of the device.

Consider first a wave incident on port 1. The energy contained in this wave is divided equally between ports A and B; none of this energy appears at port 2. The signals at ports A and B are in phase quadrature, with the signal at port A lagging that at port B as indicated. Due to the symmetry of the junction, the energy in a wave incident on port 2 will also divide equally between ports A and B; however, the signal at port B will lag that at port A by 90°. It is important to note that ports A and B are isolated hence the load on port A does not affect the power delivered to port B and vice versa. Now let us assume that simultaneously signals at the same frequency and of $\sqrt{2}\,E_1$ and $\sqrt{2}\,E_2$ amplitude are incident on ports 1 and 2. If the signals are in-phase and have equal amplitude, the signals at ports A and B will also be in-phase and have an amplitude of $\sqrt{2}\,E_1$. If the signal at port 1 leads that at port 2 by 90°, the two signals arriving at port B are 180° out-of-phase and hence vanish; at port A they add in-phase with $2\,E_1$ amplitude. Similarly, if the signal at port 2 leads that at port 1 by 90°, there is no output at port A, and all the energy exits from port B. Suffice it to say that appropriate choice of the phase difference, in the range $\pm 90°$, between signals at ports 1 and 2 will deliver any fraction of the total input power to port A or port B and the sum of the output power will be equal to the total input

power minus any power dissipated in the coupler or reflected from ports A and B. Typically, the power dissipated in the coupler (i.e., its insertion loss) $\approx$ 0.05 dB at 7.5 GHz.

A modified "magic Tee" is also a four-port device. It is customary to refer to it as having input "sum" and "difference" ports and two "output" ports. Signals incident on the sum port divide equally between the output ports and these output signals are in-phase. Signals incident on the difference port also divide equally between output ports but the output signals are 180° out-of-phase. The device is reciprocal, linear and bilateral; consequently, equal-amplitude signals incident on the output ports appear only at the sum port if they are in-phase and at the difference port if they are 180° out-of-phase. If this device is connected to the 3-dB coupler through identical phase shifters as indicated schematically in Fig. 4, signals (E_o) incident on the sum port of the magic Tee will divide between the output ports (i.e., ports A and B) in a ratio determined by

$$E_A = E_o \sin\left[\frac{(\phi-\theta)}{2} + \frac{\pi}{4}\right] e^{j\Psi} \tag{1}$$

$$E_B = E_o \cos\left[\frac{(\phi-\theta)}{2} + \frac{\pi}{4}\right] e^{j\Psi} \tag{2}$$

$$\Psi = \frac{\theta+\phi}{2} - \frac{\pi}{4} \tag{3}$$

It is also true that the insertion phase of E_A and E_B depends on the sum of ϕ and θ. Keeping the sum, $\phi + \theta$, constant, while varying the difference, $\phi - \theta$, a beam-forming network using this power dividing junction can produce an arbitrary distribution of the input power among the output ports, with no

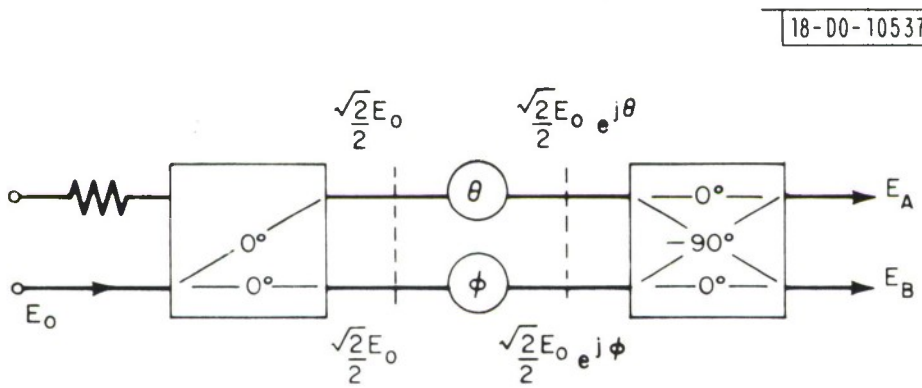

$$E_A = \frac{E_o}{2}\left[e^{j\theta} + e^{j(\varphi+90°)}\right] = E_o \sin\left(\frac{\varphi-\theta}{2}+\frac{\pi}{4}\right)\exp\left[j\,\frac{\varphi+\theta}{2}-\frac{\pi}{4}\right]$$

$$E_B = \frac{E_o}{2}\left[e^{j\varphi} + e^{j(\theta+90°)}\right] = E_o \cos\left(\frac{\varphi-\theta}{2}+\frac{\pi}{4}\right)\exp\left[j\,\frac{\varphi+\theta}{2}-\frac{\pi}{4}\right]$$

Fig. 4. Schematic representation of variable power divider.

phase variation of the output signals.

The variable insertion phase shifts, θ and ϕ, can be obtained by the use of latching ferrite phase shifters. These consist of a ferrite toroid mounted in the center of a rectangular waveguide as indicated in Fig. 5. The state of magnetization of the ferrite controls the phase shift of the signal passing through it. A single-turn control wire determines the magnetic flux density in the ferrite. The wire enters the waveguide parallel to the broad wall and hence has negligible interaction with the waveguide fields. To insure that essentially all of the r.f. energy passes through the ferrite toroid, matching end sections are used to reduce the insertion loss of the device and provide essentially reflection-free performance.

The desired insertion phase is obtained by first driving the ferrite into saturation. This establishes a "calibration" condition enabling a second drive pulse of controlled width (and amplitude) to change the flux an amount $\Delta\Psi$ to establish the desired remanent flux in the ferrite. The change in insertion phase is proportional to $\Delta\Psi$. Measured change in insertion phase of a single phase shifter and power division of a VPD are shown in Figs. 6 and 7 as a function of drive pulse width. In Fig. 7 the data was obtained by applying a pulse of width, τ, to one phase shifter (i.e., the one controlling θ in Fig. 4) and 5.05 μs-τ to the other phase shifter. This insures $\theta + \phi \approx$ constant.

IV. METHOD OF ANALYSIS

The performance of a lens antenna with a multiple-feed horn array can be calculated using physical optics and an extrapolation of measured feed

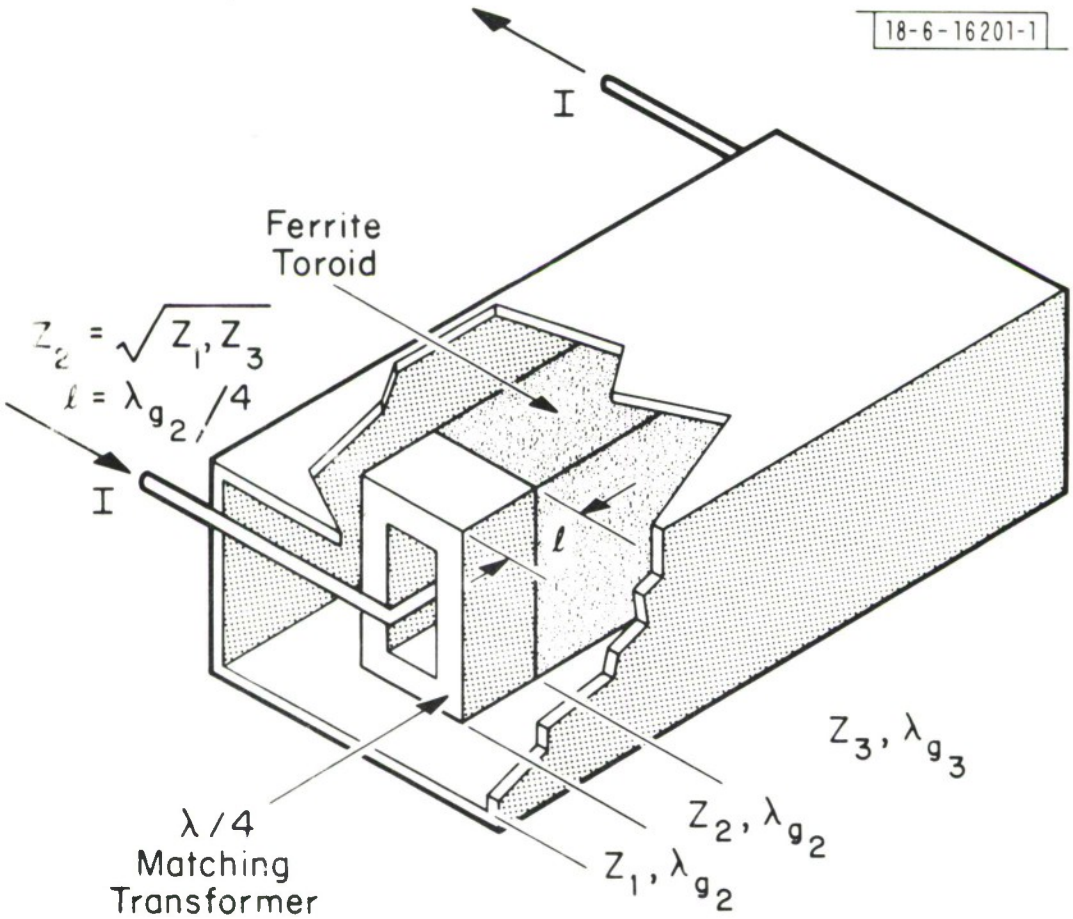

Fig. 5. Latching ferrite phase shifter

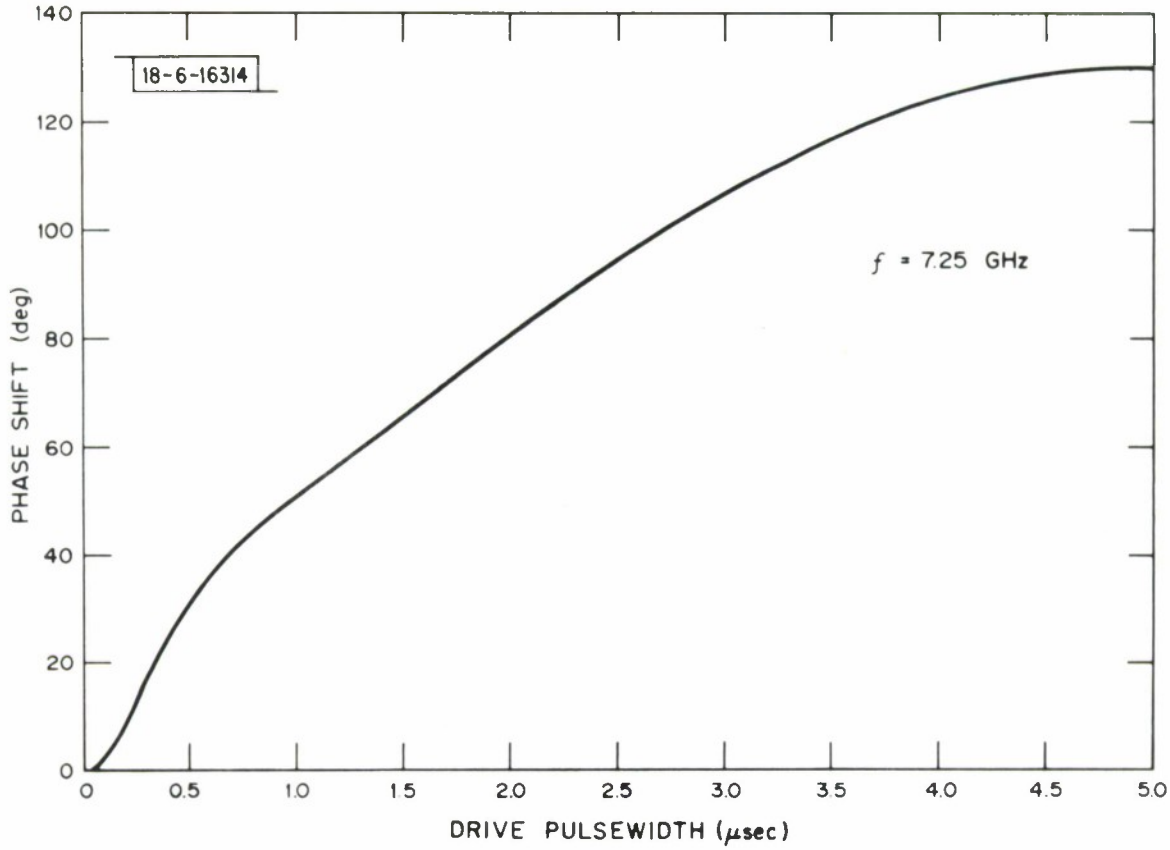

Fig. 6. Drive pulse width vs. phase shift for nonreciprocal latching ferrite phase shifter.

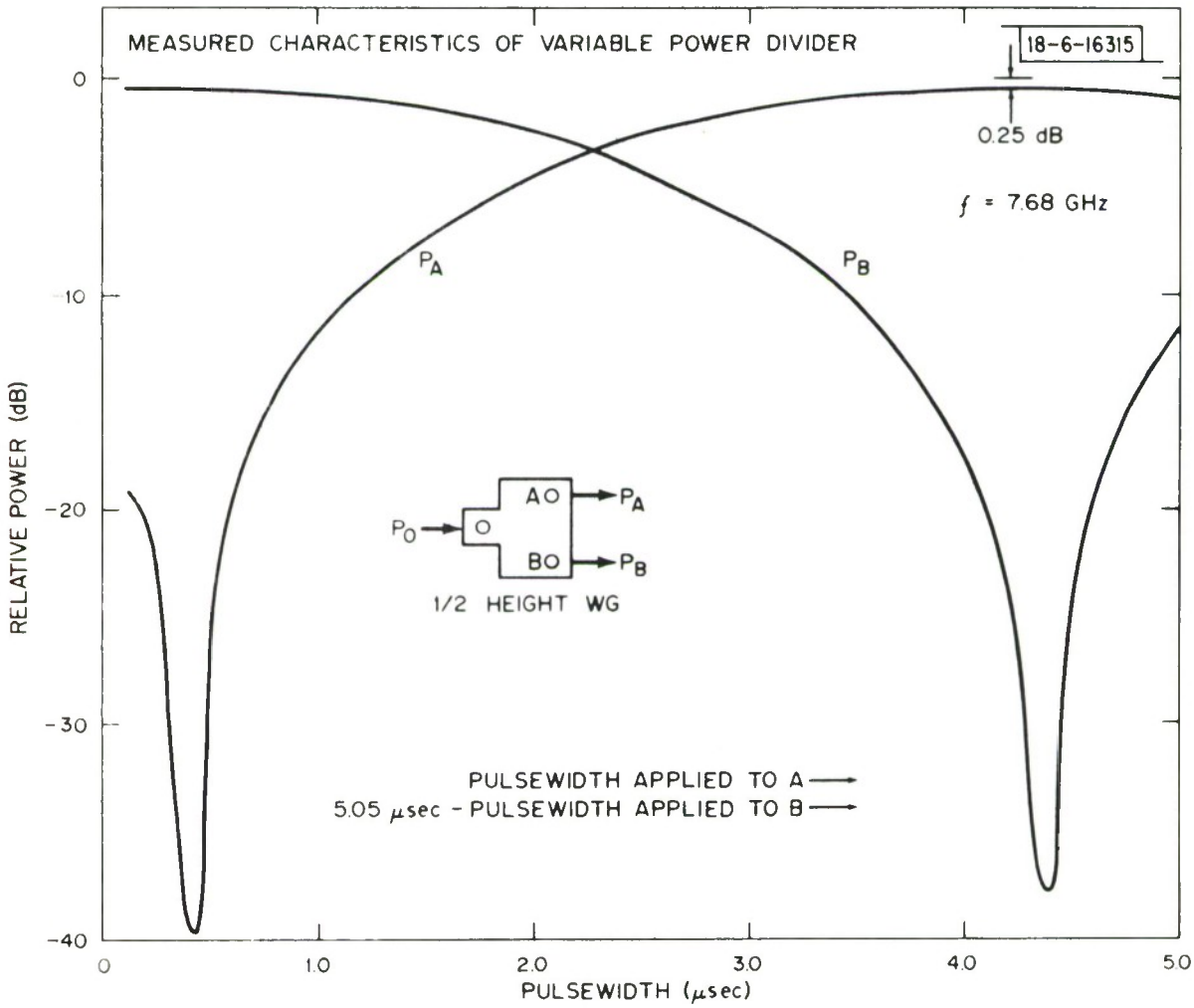

Fig. 7. Measured characteristics of variable power divider.

horn radiation patterns. Referring to Fig. 8, the waveguide lens, feed horn array and associated geometry are presented. The inner surface of the lens has a radius equal to the focal length F and a minimum thickness 0_2-0_1 at its center. The waveguides have a square cross section $\underline{a}$ on a side and are positioned by the subscripts indicating the mth row and nth column. The center line of each waveguide is located by the radius vector ρ_{mn}. The feed horn array is located in the plane z = -F and the feed horn apertures are located by the subscripts indicating the ith row and the jth element in that row.

The radiation pattern of each feed horn is represented by an analytic expression derived from measured data and known frequency behavior. The beam-forming network is shown only to indicate its location and function. The excitation of each feed horn is specified; it is assumed that the beam-forming network will produce it.

The far-zone radiation patterns are determined by calculating the physical optics field incident on the lens inner surface, the reflection and transmission at the inner and outer surface of the lens, the path length through the lens and hence the excitation of each of the individual radiating waveguide apertures. The far-zone radiation pattern is calculated by summing the contribution of each of these apertures. Although this analysis assumes the antenna is transmitting signals, identical radiation properties exist when it is receiving signals because it is a reciprocal device. However, the ferrite phase shifters used in the beam-forming network are not reciprocal and hence they cannot be used for simultaneous transmission and reception of signals. In this case, a separate beam-forming network would be required,

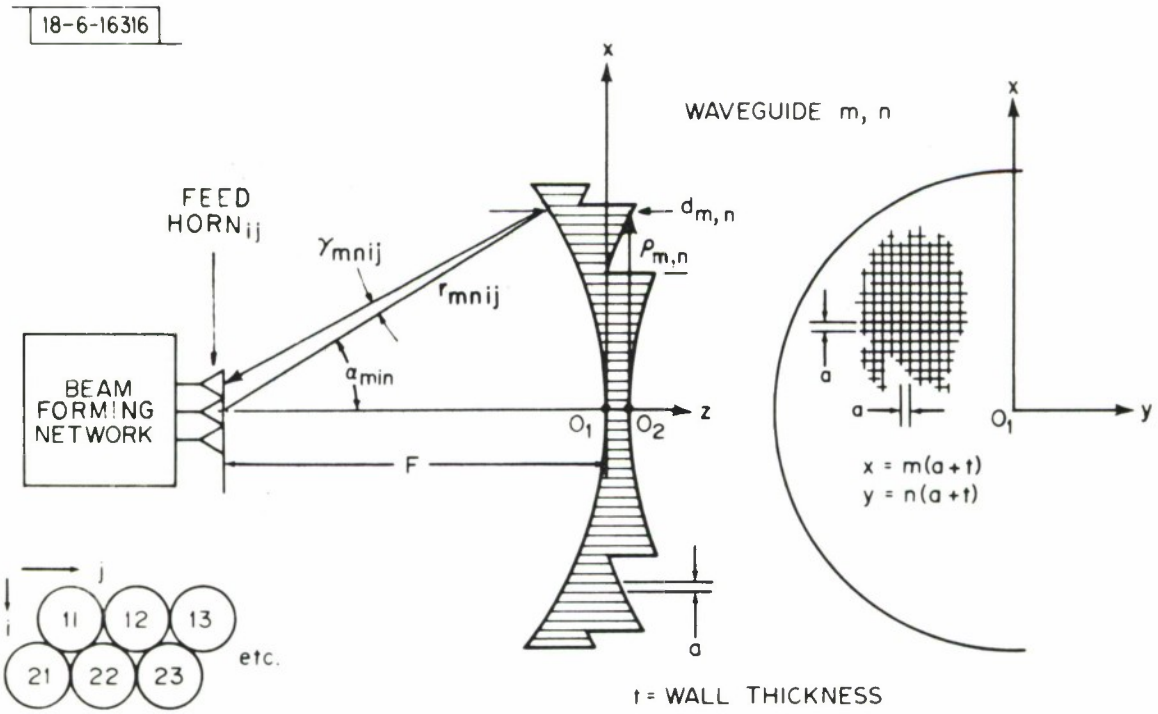

Fig. 8. Lens and feed geometry.

one for transmitting signals and one for receiving signals. The far-zone field is given by

$$G(\theta,\phi) = \frac{G_o a^4}{P_t \lambda^2 F^2} \left|E(\theta,\phi)\right|^2$$

with

$$E(\theta,\phi) = \sum_i \sum_j \sum_m \sum_n a_{ij} \frac{f \cos^{1/2}\gamma_{mnij} h(\theta,\phi) e^{-jk(r_{mnij} + \gamma d_{mn} - \vec{P}_{mn}\cdot\vec{u})}}{\frac{r_{mnij}}{F} \cos^{1/2}\alpha_{mn}}$$

where G_o = gain of a feedhorn

f = radiation pattern of a feedhorn

ν = $[1 - (\lambda/2a)]^{1/2}$ is the index of refraction of the lens

$\vec{u}$ = unit vector in the direction θ,ϕ

$h(\theta,\phi)$ = function which account for steps in waveguide lens

a_{ij} = complex excitation of feed horn ij

k = $2\pi/\lambda$

P_t = $\sum_i \sum_j |a_{ij}|^2$

and the other parameters are defined in Fig. 8.

V. MINIMUM DIRECTIVE GAIN OVER THE FIELD-OF-VIEW (FOV)

A communication system designer requires a knowledge of the directive gain of the antenna in order to establish an accurate estimate of the link margin. Directive gain is the product of the antenna directivity and its normalized radiation pattern. The designer must size the communication system for the minimum expected value of directive gain over the entire field-of-view (FOV). (FOV is the solid conical angle centered on the antenna's

focal axis, within which a prescribed minimum directive gain is realized.) With a mechanically scanned paraboloid antenna, all that is needed is knowledge of its radiation pattern and directivity. For a multiple-beam antenna the situation is somewhat more complicated. First, one must devise a means of "scanning" a beam over those angular positions between the beam directions obtained by exciting any single feed horn, for the decrease in directive gain between these beam peaks is usually unacceptable. Due to the flexibility of the variable power divider, this "scanning" can be accomplished in either a continuous or a stepwise fashion. Secondly, the change in beam shape during "scanning" must be ascertained--in general the pattern formed by exciting two or more feeds simultaneously will be different from that obtained by exciting a single feed--so that the actual coverage provided may be determined. We first analyze a stepwise method of scanning, in which either one, two or three adjacent feeds are excited, and then consider the case of continuous scanning.

1. Stepwise Scanning

It appears that a useful mode of operation of a multiple-beam antenna generating a single beam is to restrict it to a relatively simple set of controls such as excitation of one feed, or two adjacent feeds, or three adjacent feeds arranged in the form of a triangle. Assuming a FOV = 18°, which is 0.6° larger than the solid angle subtended by the earth at synchronous altitude and allows for satellite attitude variation, the minimum directive gain was calculated for operation of the multiple-beam antenna with either one, two or three feeds excited in-phase and with equal ampli-

tude. The diameter of the lens, (always keeping focal length = diameter) and the feed horn spacing were varied and the directive gain at 7.5 GHz was calculated. Since we are interested in determining the minimum value of directive gain anywhere in the FOV, it is necessary to examine two situations. These are, the minimum directive gain obtained within, and at the edge of, the field-of-view.

With a fixed lens diameter in the range 20" to 34", we start with a spacing so small (i.e., $S < \lambda$), that the FOV is less than 18°. We then increase the spacing, which <u>increases</u> the minimum directive gain on the edge of the FOV, G_e, to a maximum, G_{emax}, at a spacing $S = S_{max}$. G_e will vary between G_{emax} and $\approx 1/2\ G_{emax}$ for $S > S_{max}$ and increasing.

Considering the same initial conditions ($S < \lambda$), the minimum directive gain G_i, <u>within</u> the FOV, is larger than the gain at the edge of the FOV and <u>decreases</u> as S is increased. Hence, there exists a unique spacing, S_o, for a given lens diameter and frequency of operation, for which the minimum directive gain, G_{min}, over the entire FOV, is maximum. At this spacing $G_e = G_i$. In order to determine S_o, G_e and G_i were calculated and are plotted in Fig. 9 for various lens diameters between 20" and 34". Since S_o must be less than S_{max}, S is varied over that range which demonstrates the equality of G_e and G_i.

It is reasonable to pass a curve through all points for which $G_e = G_i$ to obtain the solid curve of minimum directive gain versus spacing. However it is necessary to recognize that for each feed spacing there exists only one lens diameter that will give the indicated G_{min}. Consequently, the plot

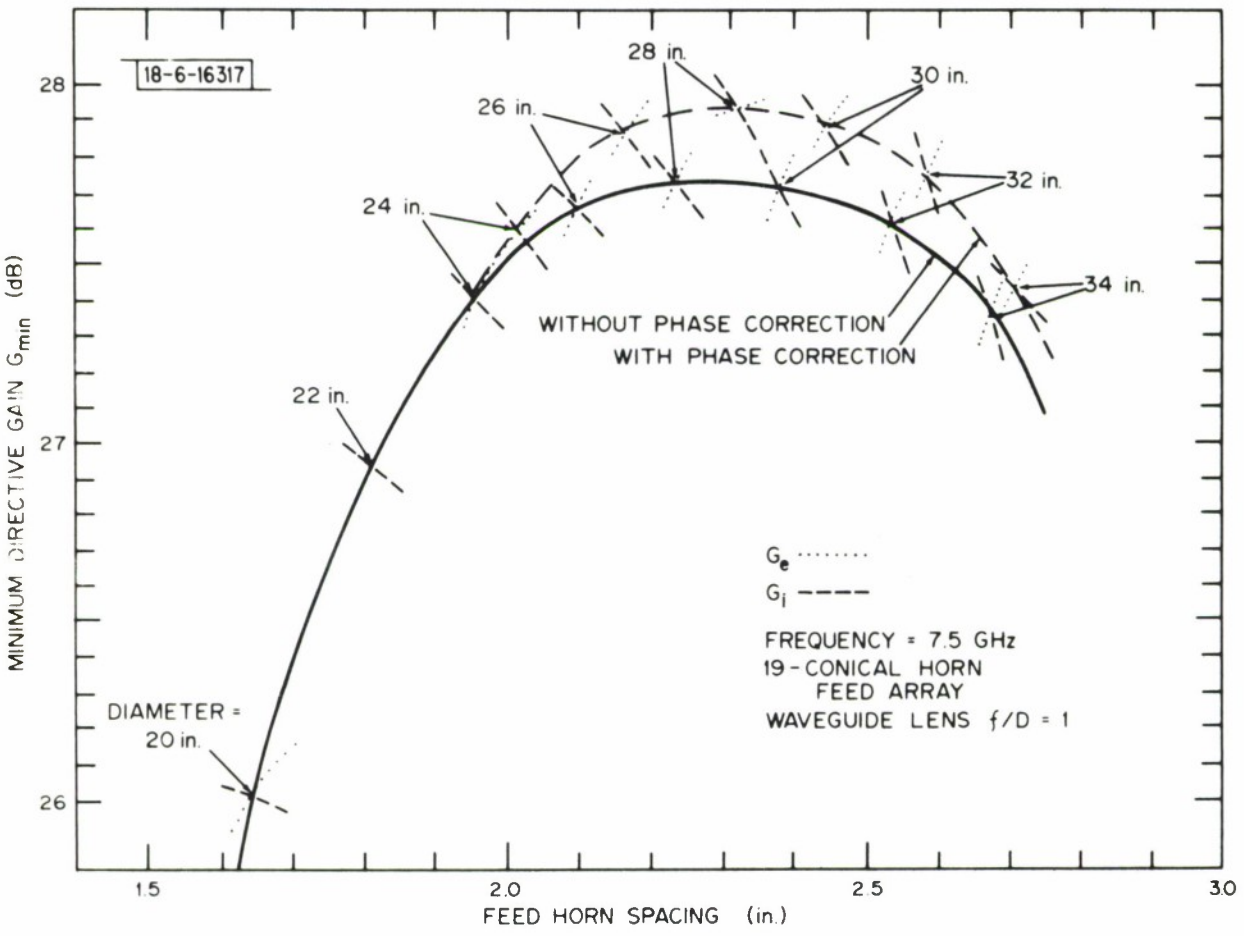

Fig. 9. Minimum directive gain over field-of-view vs. feed horn spacing.

of G_{min} versus lens diameter shown in Fig. 10 can be derived.

The data, described in the previous paragraphs of this section, were calculated for a planar array of conical feed horns. With this feed configuration, the exterior beams have a slightly different phase with respect to the center beam. Adjusting the relative phase of the signals exciting the feed horns increases the directive gain when more than one feed horn is excited simultaneously. The long dashed curve shown in Figs. 9 and 10 show this increase in G_{min} and the corresponding value S_o.

In summary, Figs. 9 and 10 show that a waveguide lens antenna illuminated by a planar array of 19 conical feed horns excited in the TE_{11} mode will have a minimum directive gain of 27.9 dB over an 18° FOV if operation is limited to the excitation of a single feed or equal distribution of input power between two adjacent feed horns or three feed horns arranged in the form of a triangle. The device is reciprocal hence the same is true when the antenna is receiving signals.

Finally, it is well recognized that the conical feed horn is not the most efficient feed to use in the assumed configuration. In particular, the aperture does not fill the hexagonal space available and its aperture field must vanish at the aperture edge in the H-plane. Hence increasing the feed horn directivity by adding an end-fire device such as a polyrod, or a traveling-wave antenna such as a yagi, or helix, etc. will result in an increase in the directive gain over the FOV. In order to investigate the effect of a more efficient feed, a hypothetical uniformly excited hexagonal aperture was assumed as the element in a 19-element feed array for the lens. It was

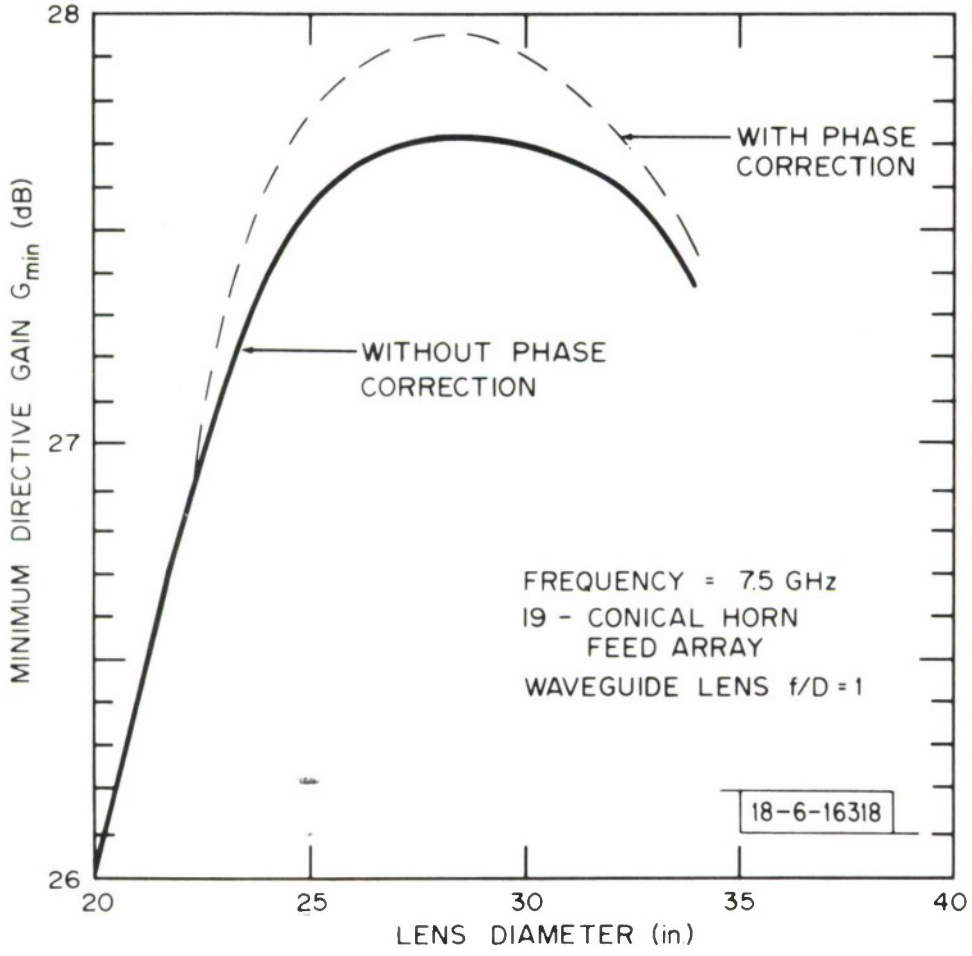

Fig. 10. Minimum directive gain over field-of-view vs. lens diameter.

felt that the gain of $4\pi/\lambda^2$ times the feed area which is obtained with this model is the maximum physically realizable gain, without incurring undesirable interaction between the feeds. The resulting minimum directive gain over an 18° FOV was calculated and is given by the lower curve plotted in Fig. 11. Notice that the maximum value of G_{min} has increased to 28.9 dB--approximately a 1-dB increase over the previous case. The corresponding maximum directivity is 32 dB. It is interesting to note that a 50% efficient 28-inch-diameter paraboloid operating at the same frequency also has a directivity = 32 dB. The added flexibility of the multiple-beam antenna does not compromise its directivity, it is the losses in the beam-forming network which compromise its gain.

The nature of the coverage obtained by exciting either one feed horn, or two or three simultaneously so as to maximize G_{min} is demonstrated in Fig. 12. The solid curves shown represent the directive gain contours corresponding to the excitation of a single uniformly illuminated hexagonal cell located at feed horn positions 31, 32 or 21. The dotted contour corresponds to the simultaneous and equal excitation of two adjacent cells located at 31 and 32, 31 and 41, 21, 32 and 21. The dashed contour is obtained when all three cells are excited simultaneously and with equal-amplitude signals. All contours represent a directive gain of 28.9 dB; the directive gain within any closed contour is > 28.9 dB. The directive gain over most of the triangle (shown in by the dash-dot lines) is > 30 dB. The edge of the 18° FOV is indicated by a dashed line.

Before leaving this subject it may be of interest to note the results

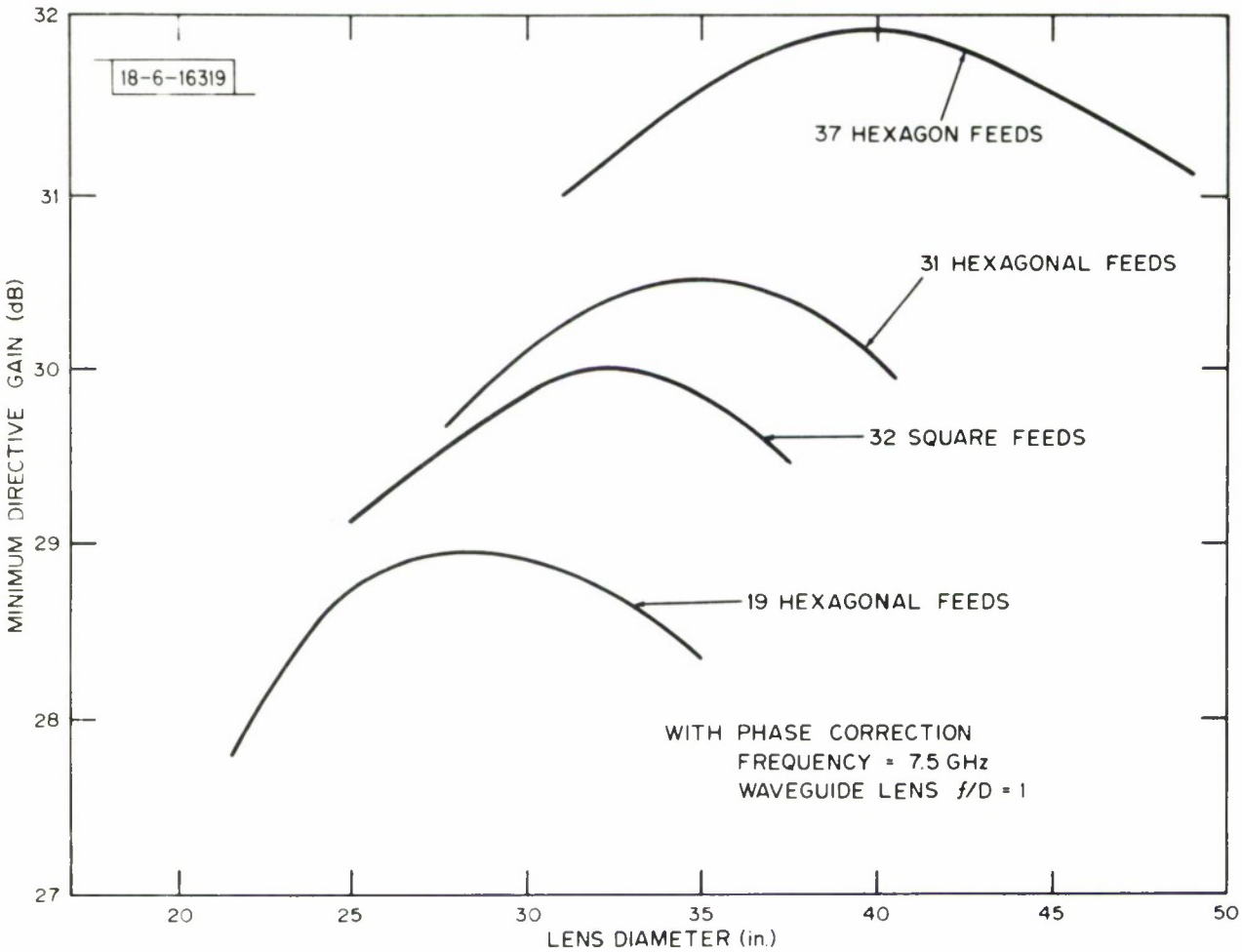

Fig. 11. Minimum directive gain vs. lens diameter for various feed clusters.

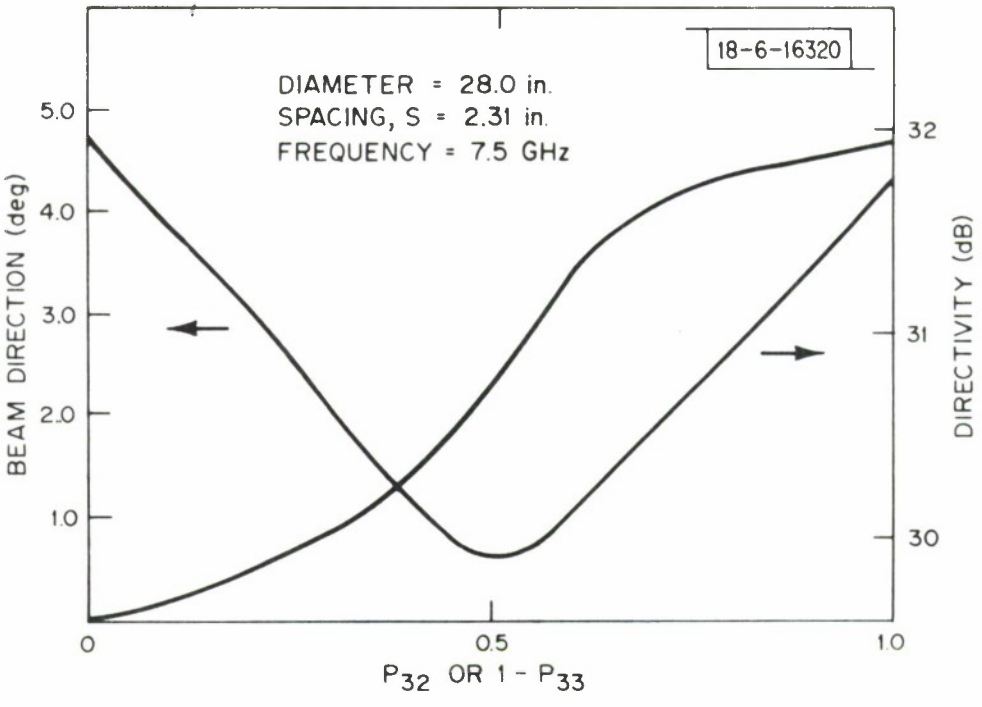

Fig. 12. Continuous beam scanning characteristics.

obtained when the 19-hexagonal feed element array is enlarged to a 37-hexagonal feed array. The minimum directive gain obtained by exciting one, two or three feeds varies with lens diameter as indicated by the upper curve in Fig. 11. The maximum value of G_{min} increases ≈ 3 dB and the corresponding lens diameter is 40 inches (an increase of 43%), as would be expected.

Because the desired FOV is circular, one might suggest removing the six feed elements located at the ends of the three seven-element rows of a hexagonal 37-element feed, because their beams lie partly outside the circle. Alternatively, one might consider arranging 32 feed elements on a square grid of six rows and six columns with the corner feed elements removed. Limiting operation, in the latter case, to excitation of one, two or four feed elements, and to one, two or three feeds in the former case, G_{min} was calculated. The variation of G_{min} with lens diameter is plotted in Fig. 11 for further comparison. Of particular interest is the superior performance obtained when the feed elements are hexagonal and arranged on a triangular instead of a square lattice.

2. Continuous Beam Scanning

In this section we illustrate the calculated beam scanning performance obtained by varying the power distribution in a continuous fashion between two adjacent feed horns. Let us consider the radiation patterns obtained when two circularly polarized adjacent hexagonal feed cells, say cell No. 32 and No. 33, are excited in-phase with the total input power held constant. We are particularly interested in the beam direction and antenna directivity as P_{32} the power delivered to feed horn No. 32 is varied from 0 to 1 while

the power P_{33} delivered to horn No. 33 is varied as $1 - P_{32}$. Let us assume the same lens that is found to be optimum for stepwise scanning, i.e., a 28.0-inch-diameter lens (focal length = 28 inches) operating at a frequency of 7.5 GHz with a feed spacing S = 2.31 inches, a horn aperture diameter = 2.31 inches and a lens made up of square waveguides 0.995 inch on a side, and calculate the directivity and radiation pattern using the method described previously. The desired information is summarized in Fig. 13 where directivity and beam direction are given as a function of P_{32} and $1 - P_{33}$. The directivity varies ≈ 2.0 dB and the half-power beamwidth of the radiation pattern varies from $\approx 3.6°$ to $7.2°$. (The reader should be cautioned that the minimum directivity shown in this figure is greater than the minimum value of directive gain that would be obtained over the FOV by scanning the beam in this manner because at least three feeds, instead of two, would have to be used to cover the FOV.) The maximum sidelobe level remains at about the same level; i.e., 22 dB below the peak of the main beam.

Decreasing the spacing from 2.31 inches (1.47λ) to 1.89 inches (1.2λ) reduces the variation in directivity as the beam is scanned from one extreme position to the other and also makes the curve of beam direction vs P_{33} more linear. However, reducing the spacing between feed horns decreases the field-of-view. With S = 1.47λ, the FOV is $\approx 18°$. In order to achieve the same FOV with 1.2λ spacing, the lens diameter would have to be reduced to $\approx$ 23 inches which would reduce the directivity. This may, nevertheless, result in an increase in the minimum directive gain over the FOV; an appropriate study would be required to ascertain the effect of varying these

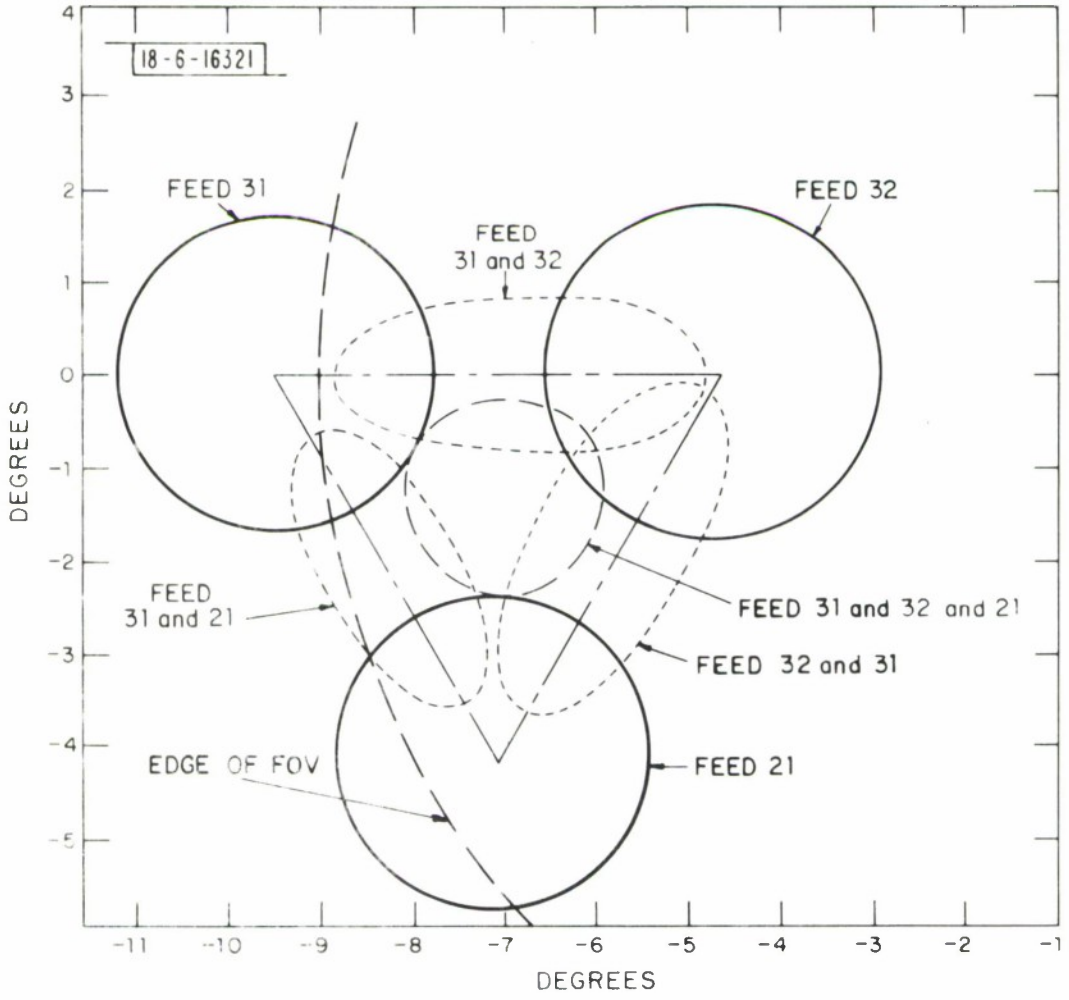

Fig. 13. 29.3 dB radiation contours for indicated feeds excited.

parameters in the same manner as was done in the stepwise beam scan described in the previous section.

In conclusion, continuous beam scanning is possible, and may increase the minimum value of directive gain over that achievable by exciting one, two adjacent, or three adjacent feeds. A detailed presentation of the actual increase in directive gain is beyond the scope of this note. Preliminary calculations indicate that a 0.3-dB increase is possible. This improvement must be weighed against the added control commands that would be required.

VI. EARTH-COVERAGE PATTERN WITH PRESCRIBED MINIMA

The use of multiple-beam antenna systems in the receiving mode on communication satellites is often justified by the need to suppress interfering signals by radiation pattern shaping. A particularly useful radiation pattern shape is one which provides uniform coverage of that portion of the earth's surface which is visible to the satellite with exception of the points where interfering signals originate. Since, in a practical sense, only a finite reduction in the antenna's directive gain in the direction of the interfering source can be realized, the title of this section is a logical description of that radiation pattern which will produce the intended discrimination. The following is a description of methods, to realize such patterns, which are well within the state-of-the-art.

1. Obtaining Minima by Turning Off Selected Feed Horns

This analysis assumes circular polarization, hexagonal feed horn apertures spaced 2.1 inches, lens diameter = 26 inches and frequency = 8.15 GHz. The horns are arranged in a triangular lattice and the earth-coverage radiation contour plot obtained with all

feeds excited with equal amplitude and in-phase is shown in Fig. 14a. This lens and feed were designed to produce an 18° FOV which is indicated by the dashed line. Increasing the amplitude of excitation of six feeds in the outer ring 2.8 dB more than all other feeds improves the earth-coverage pattern by making it conform more closely to the desired circular FOV. In particular increasing the excitation of feeds numbered 12, 21, 24, 41, 44 and 52 produces the radiation contour plot shown in Fig. 14b. The -2-dB contour conforms very closely to the edge of FOV. The minimum directive gain is increased $\approx$ 0.7 dB and the lower directive gain is mostly over the center of the FOV.

The earth-coverage radiation pattern with prescribed minima (ECPMIN) is obtained by exciting all feed horns except those which produce beams pointing in the direction of the interfering source or sources. When the source falls between two or three adjacent beams it is necessary to "turn off" those two or three beams to produce the desired spatial discrimination. (We will consider the antenna as transmitting signals; since it is a reciprocal device the same "radiation" pattern exists when it is receiving signals.) In order to determine the effectiveness of this method of forming an ECPMIN, contour plots of radiation patterns obtained by the excitation of all but one or two or three adjacent feeds were calculated. For example, excitation of all but feed horn No. 23 produces the contour plot shown in Fig. 15. The contours are shown for directive gain of 0, 1, 2, 3, 4, 5, 10, 15, 20, 25 and 30 dB below the antenna directivity indicated in the figure. This feed excitation produced a minimum $\approx$ 22 dB below the antenna directivity (i.e., peak value of

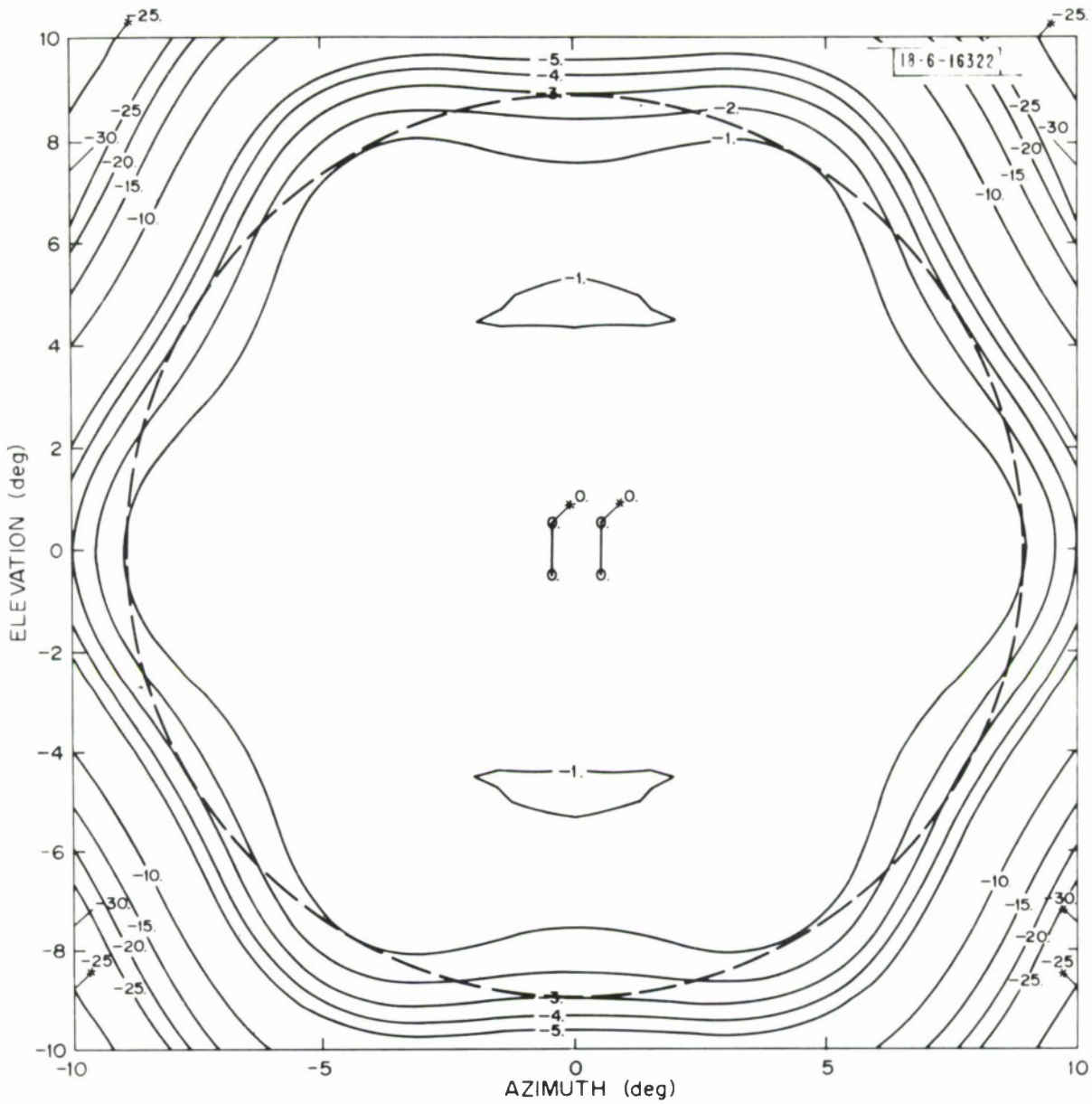

Fig. 14a. Earth-coverage pattern contours, all feeds excited equally (Directivity = 21.2 dB).

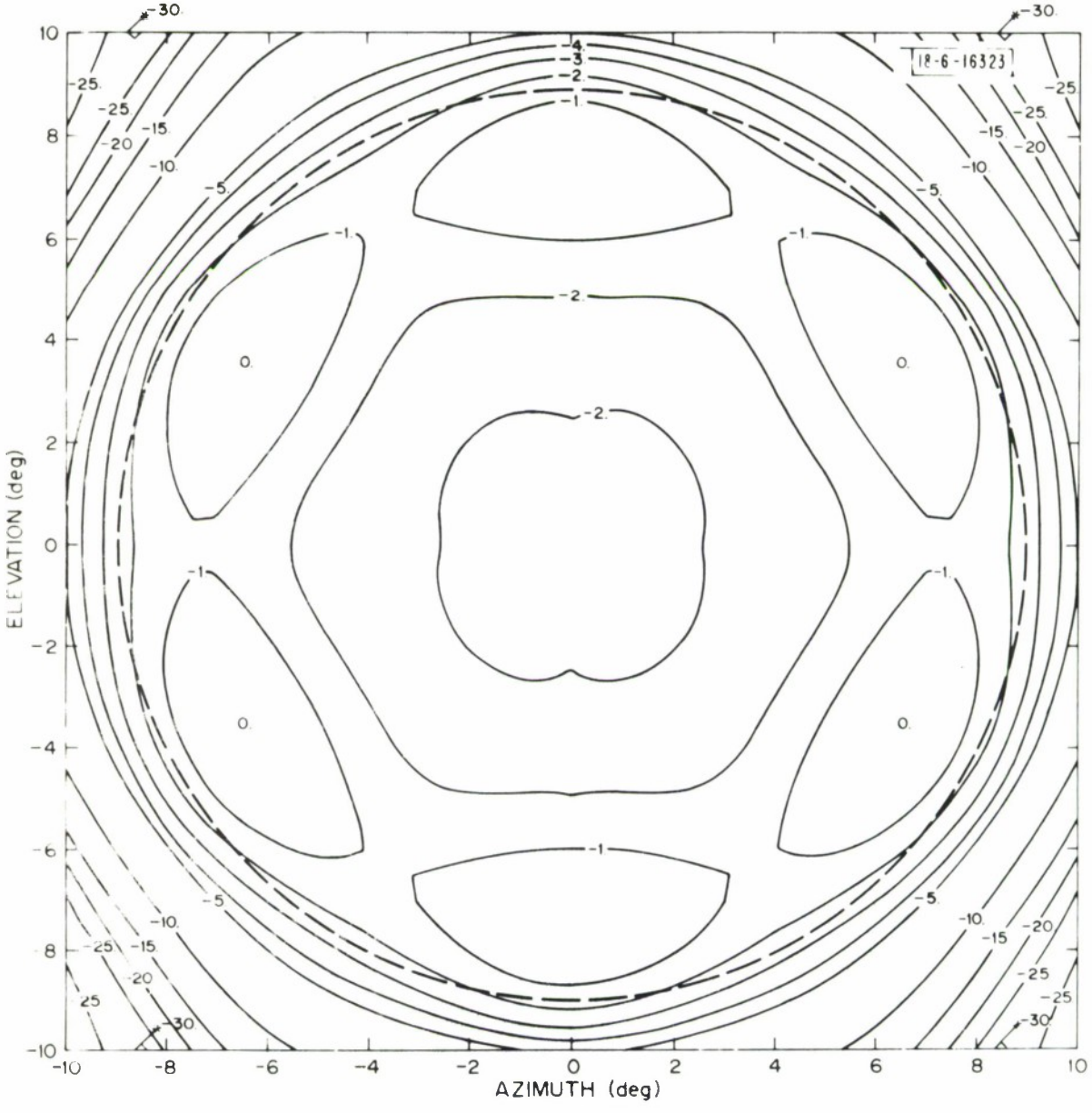

Fig. 14b. Earth-coverage pattern contours, selected feeds excited more strongly (Directivity = 21.6 dB).

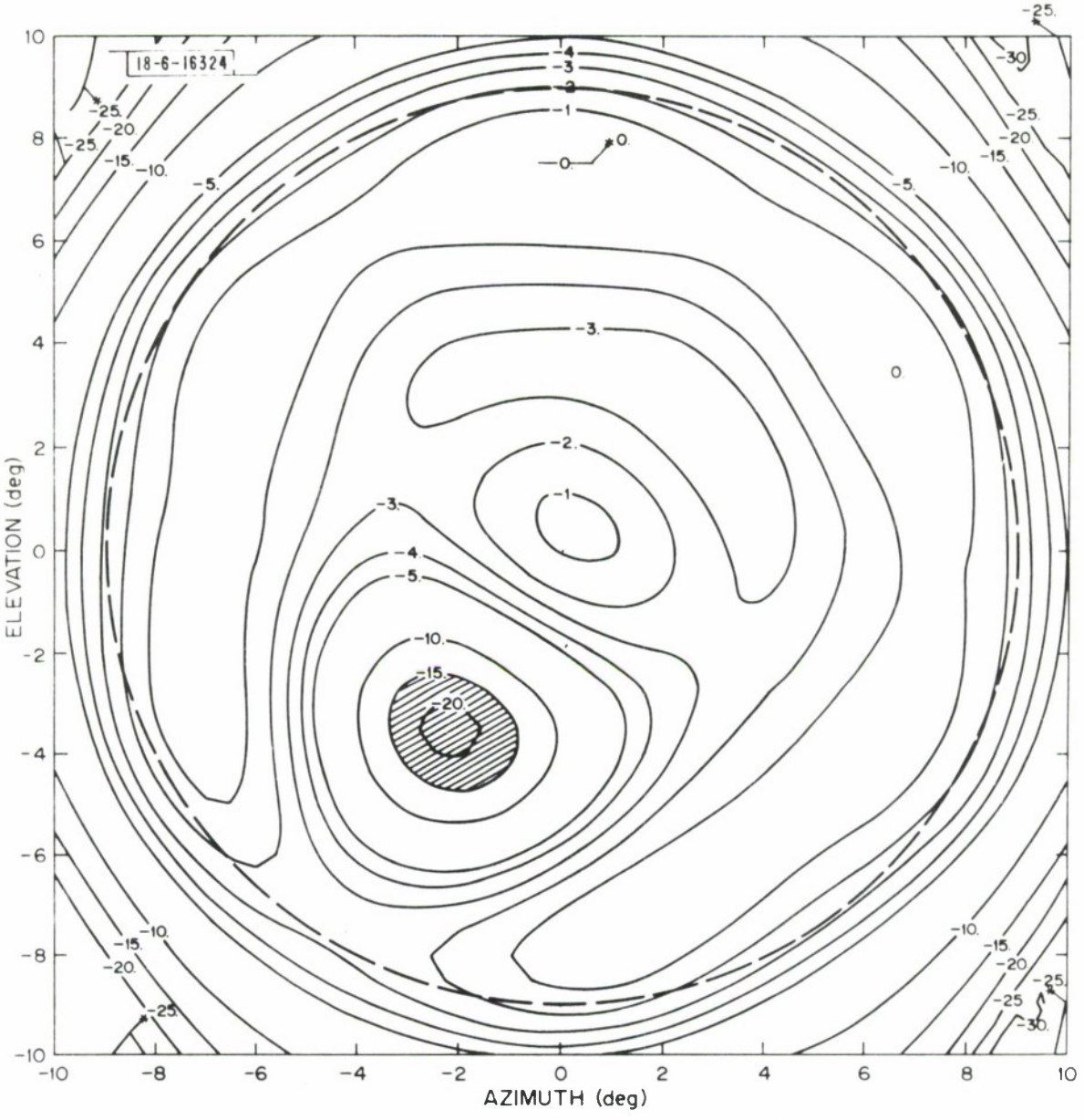

Fig. 15. Earth-coverage pattern with one beam turned off (Directivity = 21.9 dB).

directive gain). An area corresponding to a $\geq$ 15-dB reduction in directive gain has been cross-hatched to emphasize its existence.

Similar plots with each of the other six feed horns located in the upper left-hand quadrant turned off, one at a time, were calculated and a composite representation of these minima is shown by the solid areas in Fig. 16 which indicates that this technique alone is not capable of producing a $\geq$ 15-dB reduction in directive gain at every point in the FOV.

If all but two adjacent feed horns are excited, the angular area of the minimum is approximately doubled and it includes essentially the composite angular area of the minima created by turning off either of the feeds separately and that angular area joining them. For example, when all except feed horns numbered 22 and 23 are excited, the radiation contour is as indicated in Fig. 17. Similarly radiation contours were calculated by successively turning off the remaining pairs of feed horns located in the upper left quadrant of the array. A composite presentation of the areas with $\geq$ 15 dB reduction in directivity similar to that shown in Fig. 16 is best represented by showing only those areas where a $\geq$ 15-dB reduction in directive gain was not obtained. That is the small dotted angular area about the satellite's nadir position and the 6 cross-hatched areas indicated in Fig. 16. Reduction in the directive gain over the 6 cross-hatched areas can be produced by turning off corresponding triangular clusters of feeds. A contour plot of the radiation pattern when the triangular feed horn cluster 21, 31, 32 is turned off is shown in Fig. 18.

Unfortunately, it is not possible to produce a $\geq$ 15-dB minimum over the

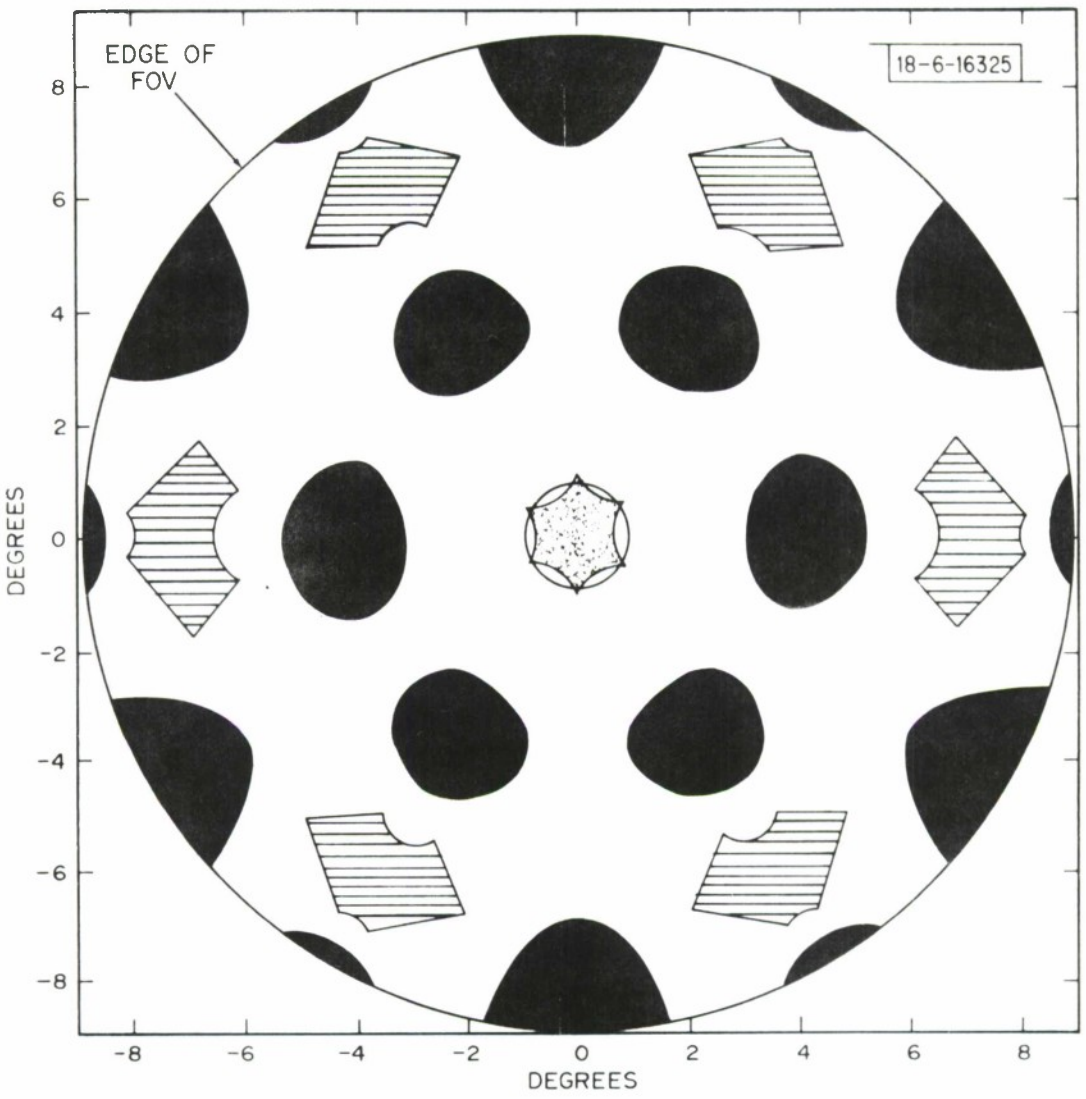

Fig. 16. Composite earth-coverage pattern with nulls.

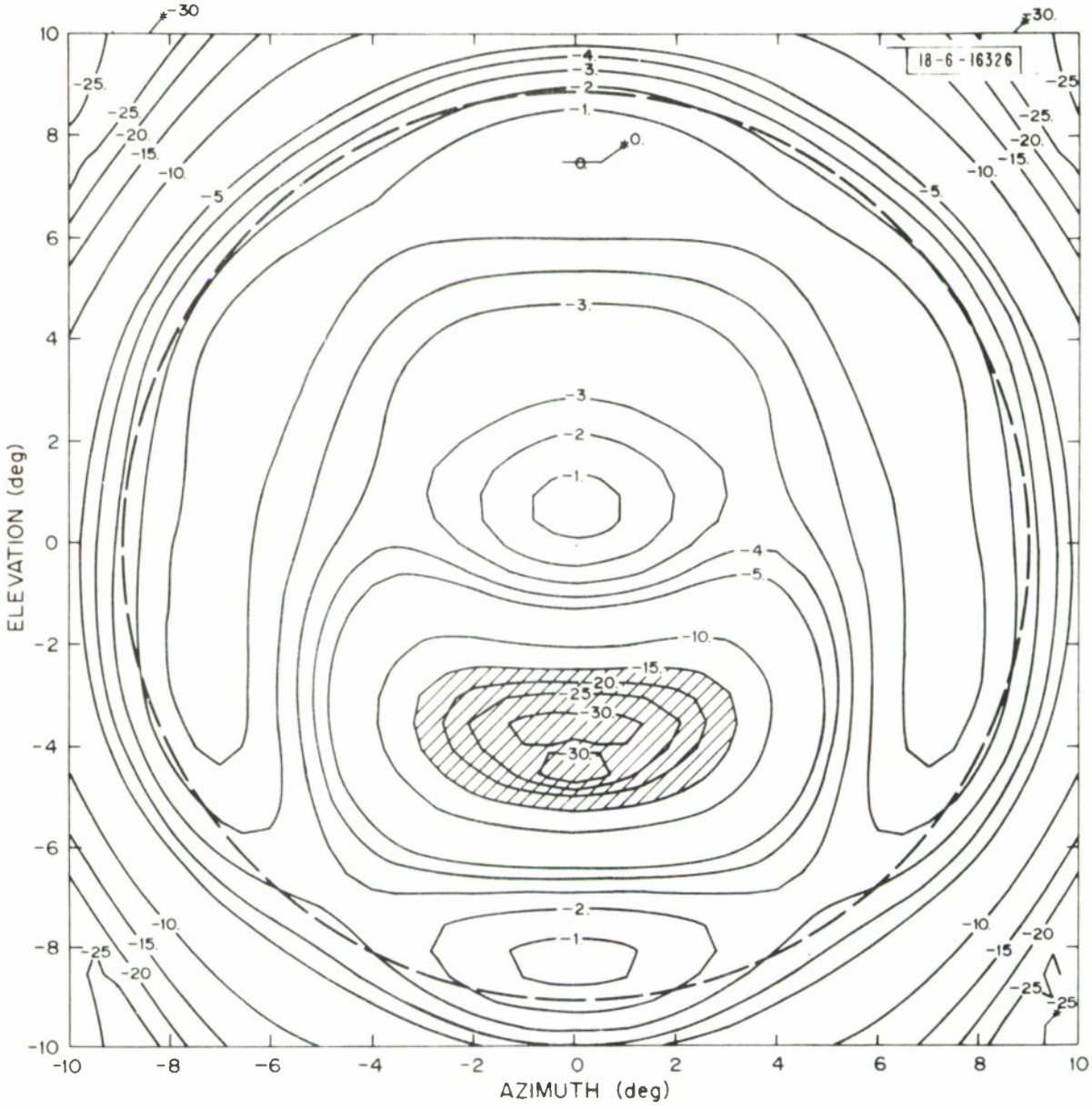

Fig. 17. Earth-coverage pattern with two beams turned off (Directivity = 22.3 dB).

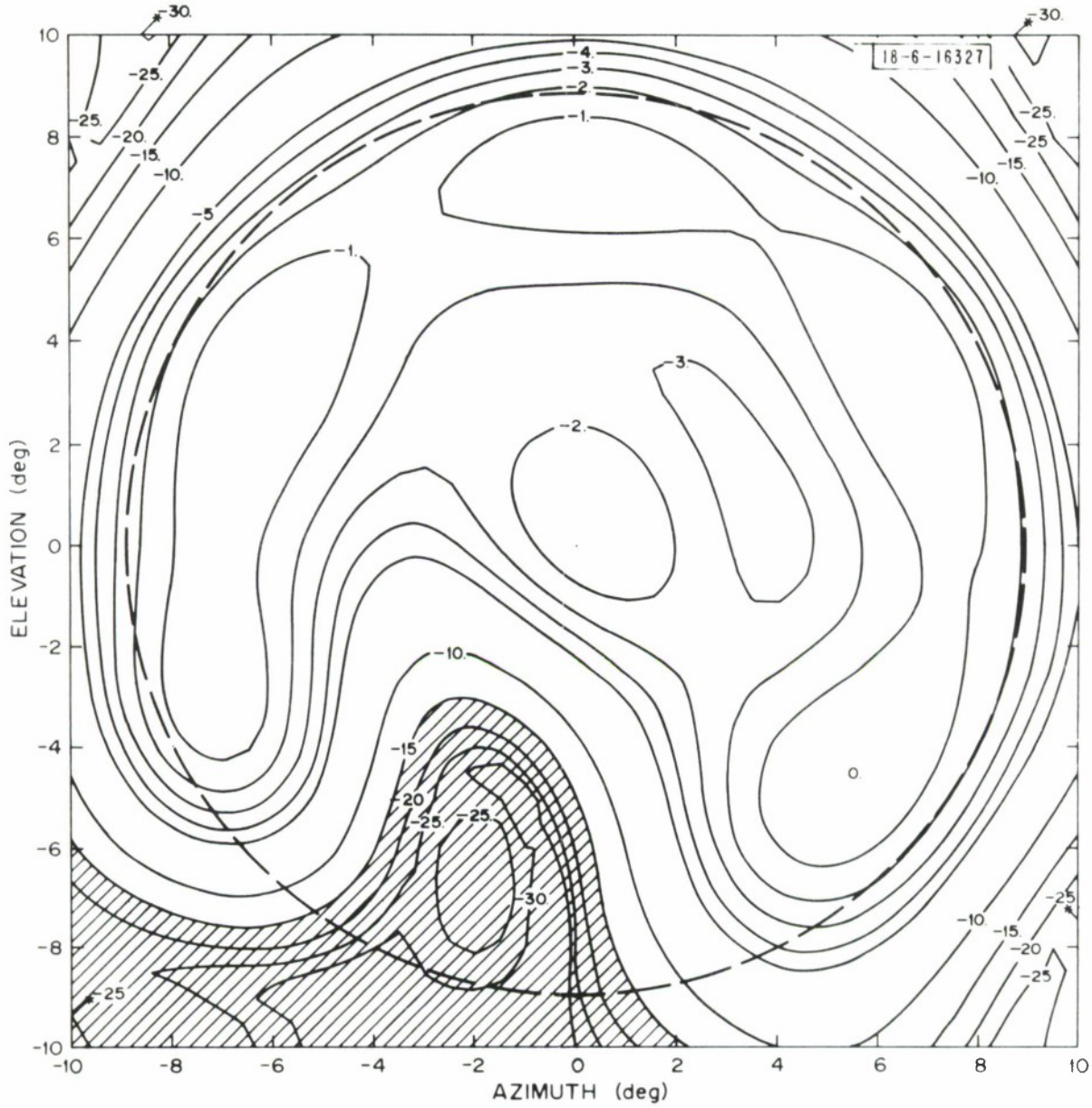

Fig. 18. Earth-coverage pattern with three beams turned off (Directivity = 22.5 dB).

small dotted area centered on the satellite's nadir by merely turning off any combination of one, two or three feed horns. However, if the center horn (No. 33) is excited 180° out-of-phase with the remaining 18 and with a relative amplitude ≈ 0.25, a $\geq$ 15-dB reduction in directive gain (indicated by the solid circle shown in Fig. 16) can be produced in the center of the field-of-view.

In summary, the foregoing set of calculated data demonstrates that an earth-coverage pattern with prescribed minima can be realized by merely turning off one, two adjacent or three adjacent feed horns. Referring to Fig. 16, a signal originating from the direction corresponding to the solid darkened angular areas can be reduced by at least 15 dB if the single feed horn most tightly coupled to this signal is turned off. If the signal originates from an angular direction corresponding to the blank angular area within the FOV, it can be reduced by $\geq$ 15 dB by turning off the two appropriate feed horns. Signals originating in the cross-hatched areas can be reduced $\geq$ 15 dB by turning off the three appropriate feed horns. If the undesirable signal originates from a direction within 0.2° of the satellite's nadir position, the signal can be reduced $\geq$ 15 dB by exciting the center feed 180° out-of-phase with the remaining feeds and with a relative amplitude ≈ 0.25.

This method of producing minima in an earth-coverage radiation pattern is straightforward, within the state-of-the-art and can be accomplished with very little complexity of control. It has the disadvantage of reducing the directive gain over an area that is sometimes larger than necessary in order to reduce the directive gain in the desired directions (i.e., when three

feeds must be turned off to reduce the signal). This can be avoided at the expense of some additional complexity, by "steering" the "null" in a manner analogous to steering beams as described in an earlier section of this note. This method will be described and discussed in the next section.

2. Null Steering

An earth-coverage pattern with prescribed minima can be obtained if the multiple-beam antenna is excited such that all except two adjacent feed horns are excited with in-phase and equal-amplitude signals, say 0° and 1 volt, respectively. The remaining two adjacent feed horns, say 31 and 32, are excited with -90° and +90° relative phase, respectively. By varying their relative excitation between 0 and 1 volt a minimum in the radiation pattern can be made to move from the direction obtained with feed horn No. 31 turned off to that obtained with feed horn No. 32 turned off.

In order to demonstrate this method, the radiation contours of a 26.0-inch-diameter lens (f/D = 1) operating at 7.5 GHz and illuminated by a 19-element hexagonal feed horn array were calculated. The antenna was designed to have an 18° FOV and the initial earth-coverage pattern without prescribed minima was obtained by increasing the relative excitation amplitude of feed horns numbered, 12, 21, 24, 41, 44 and 52 as before to improve the shape of the earth-coverage pattern.

Feed horns 21 and 22 were excited with +90° and -90° phase relative to the remaining feeds.* With the ratio of power into feed horn No. 21 to that

*It was also necessary to incorporate the phase correction, described earlier, which "converts" the planar array of feeds to feeds located on the surface of a sphere centered on the vertex of the lens.

into feed horn No. 22, P_{21}/P_{22}, set successively to 0, 0.1, 1, 10, ∞, the radiation contours over the FOV were calculated. The composite angular area over which the directive gain is reduced by at least 15 dB is indicated by the dashed curves in Fig. 19. A similar set of data with feed horns No. 32 and No. 21 instead of feed horns No. 21 and No. 22 is represented by the dotted curves in Fig. 19. The solid curves in Fig. 19 define the areas that result with feed horns No. 22 and No. 31 instead of No. 21 and No. 22. From this composite representation we see that a greater than 15 dB reduction in directive gain can be realized over the triangular area defined by the beam axes of the single excitation of feed horns No. 31, 32, and 21. Consequently, this "null" steering method can be used to produce a greater than 15 dB reduction in directive gain anywhere in the FOV.

A contour plot of the radiation pattern obtained when $P_{31}/P_{32} = 1$ is shown in Fig. 20. Note that the angular area, where the directive gain is reduced by at least 15 dB, is approximately equal to that when a single feed is turned off as indicated by Fig. 15. Null steering thus sacrifices less coverage than does turning off two or three beams to achieve a minimum.

VII. EXPERIMENTAL RESULTS

1. Radiation Patterns

The calculated data presented in the previous sections of this note would be of little value without experimental confirmation of their accuracy. For this reason, the radiation characteristics of the antenna shown in Fig. 1 were measured and compared with corresponding calculated results. For example, the H-plane radiation pattern obtained when only feed horn No. 33

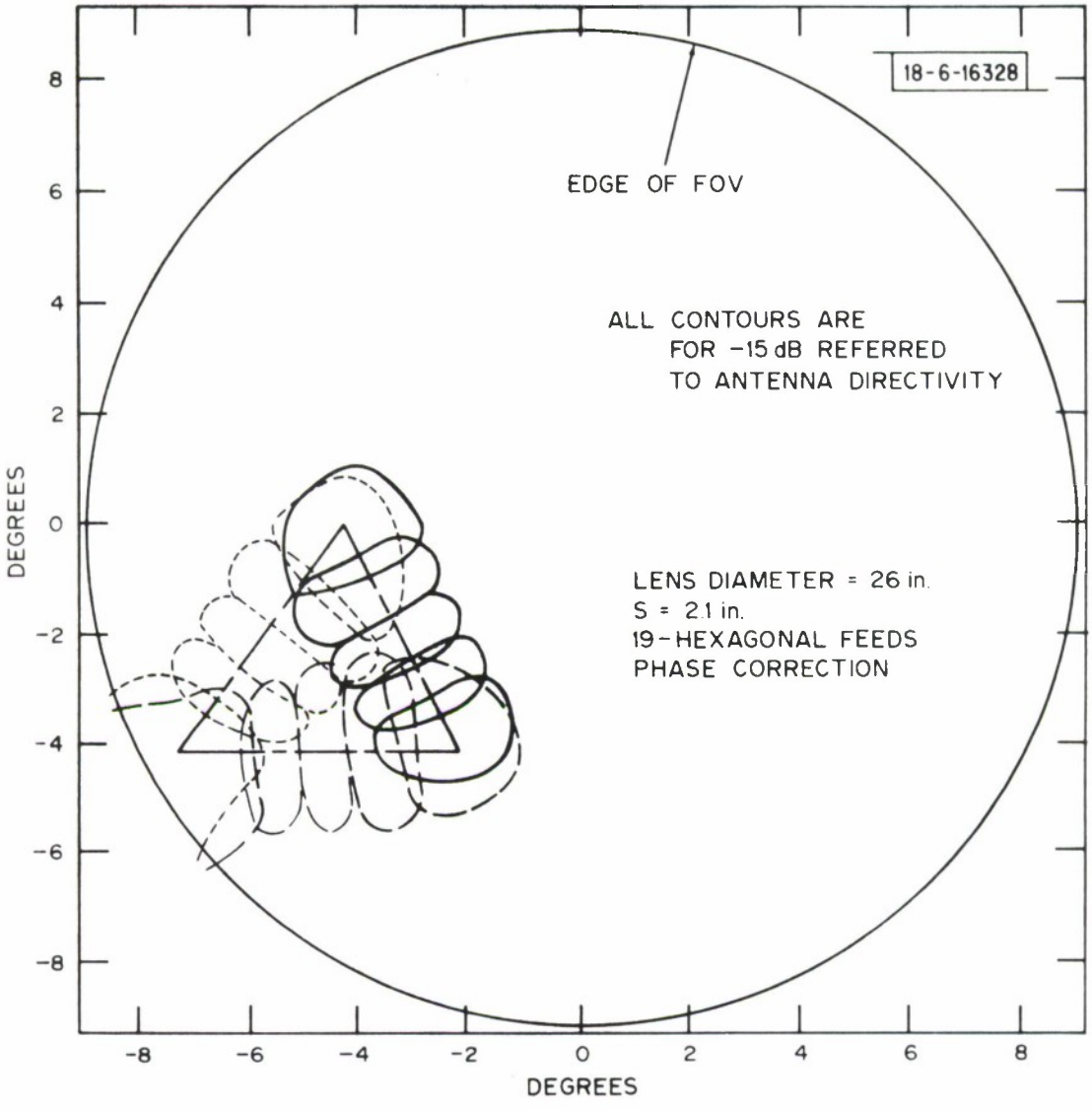

Fig. 19. Composite radiation patterns for null steering.

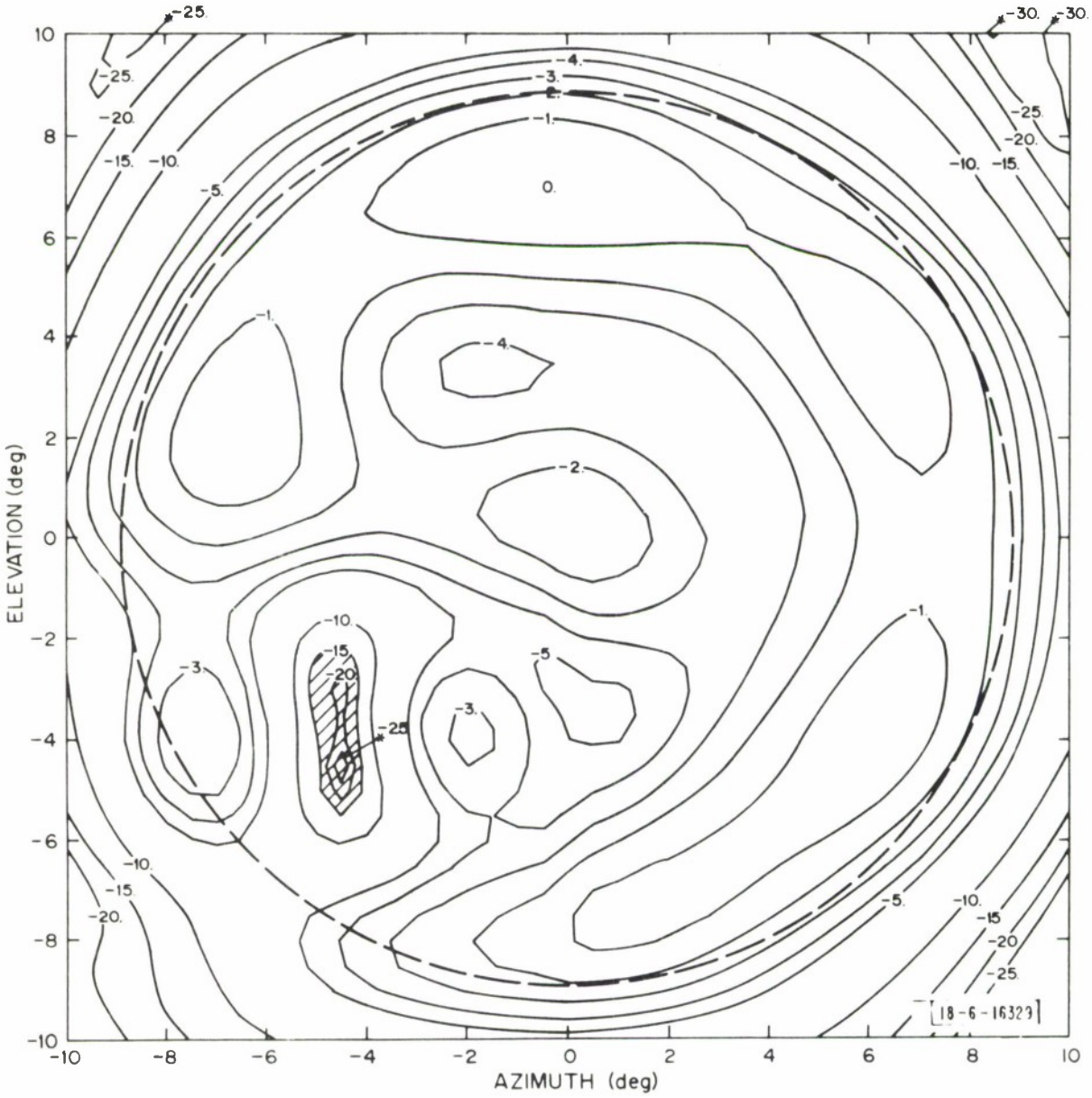

Fig. 20. Earth-coverage pattern with two feeds at 90° and -90° relative phase (Directivity = 22.0 dB).

is excited is shown in Fig. 21. The dashed curve is the calculated pattern. Similar E- and H-plane patterns were measured with only Feed No. 31, 32, 22 or 11 excited. In all cases the first sidelobe maxima were within 1 dB of their calculated values and the measured beam direction, half-power beamwidth and null position were in extremely good agreement with the calculated results.

When calculating radiation characteristics the "phase center" of the assumed feed horn or feed element is known or at least postulated. This cannot be done for the experimental model since the horn's center of phase is not known prior to assembly with the lens. Consequently, it is usually necessary to "focus" the feed array by changing x_o, the separation, measured parallel to the focal axis, between the feed horn aperture and the vertex of the lens. The measured and calculated directivity, with feed horn No. 31, 32 or 33 excited, one at a time, is shown in Fig. 22. Note that measured and calculated values are within 0.2 dB except for horn No. 33 where the difference is as large as 0.5 dB. The agreement is good since the accuracy of the measured values is only within $\approx$ 0.4 dB. The relative variation in directivity is in much better agreement except again for the case of the center feed horn (i.e., No. 33). This moderate disagreement can be explained as an interaction between the center feed horn and energy reflected from the inner surface of the lens. It does not occur for the other feed horns because in their case the energy reflected from the inner surface of the lens is not as well "focused" and it is returned to another feed horn. Nevertheless the agreement indicates that the analytic model is sufficiently accurate

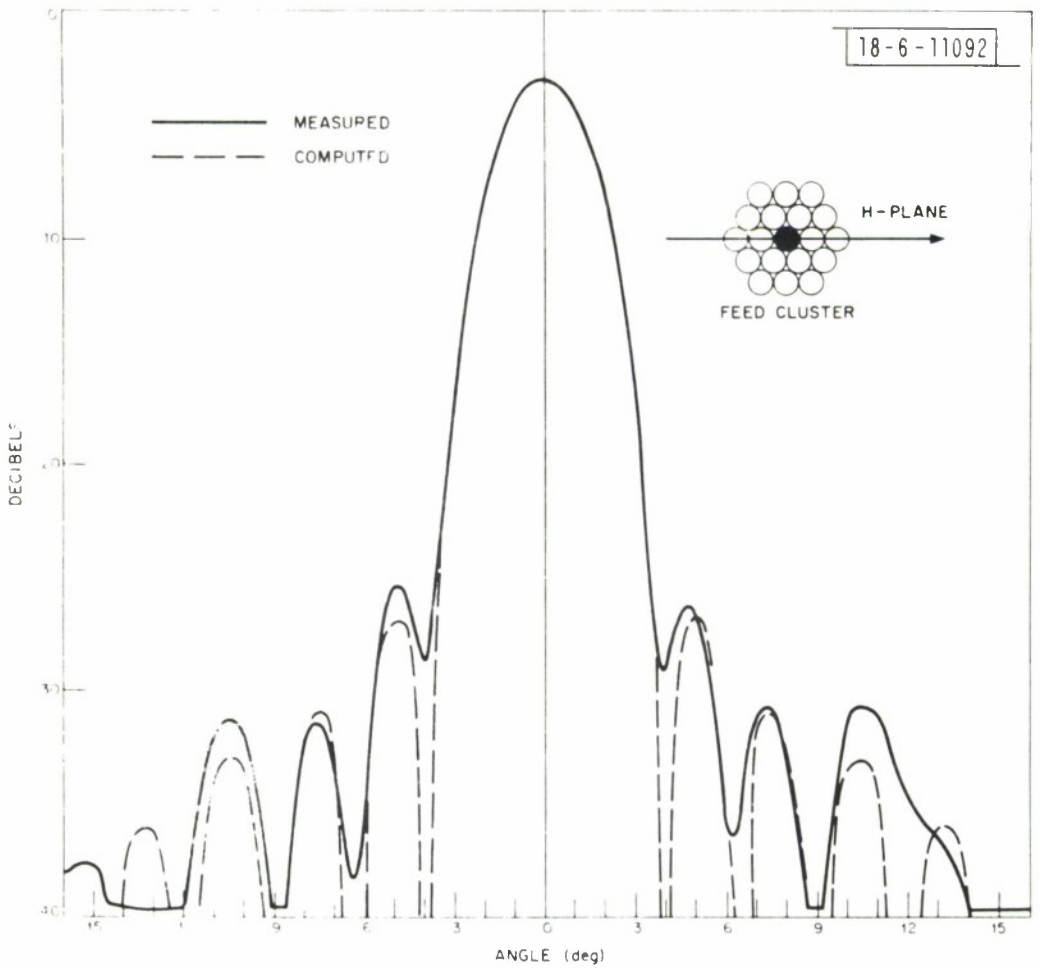

Fig. 21. Comparison of measured and computed H-plane pattern, single feed excited.

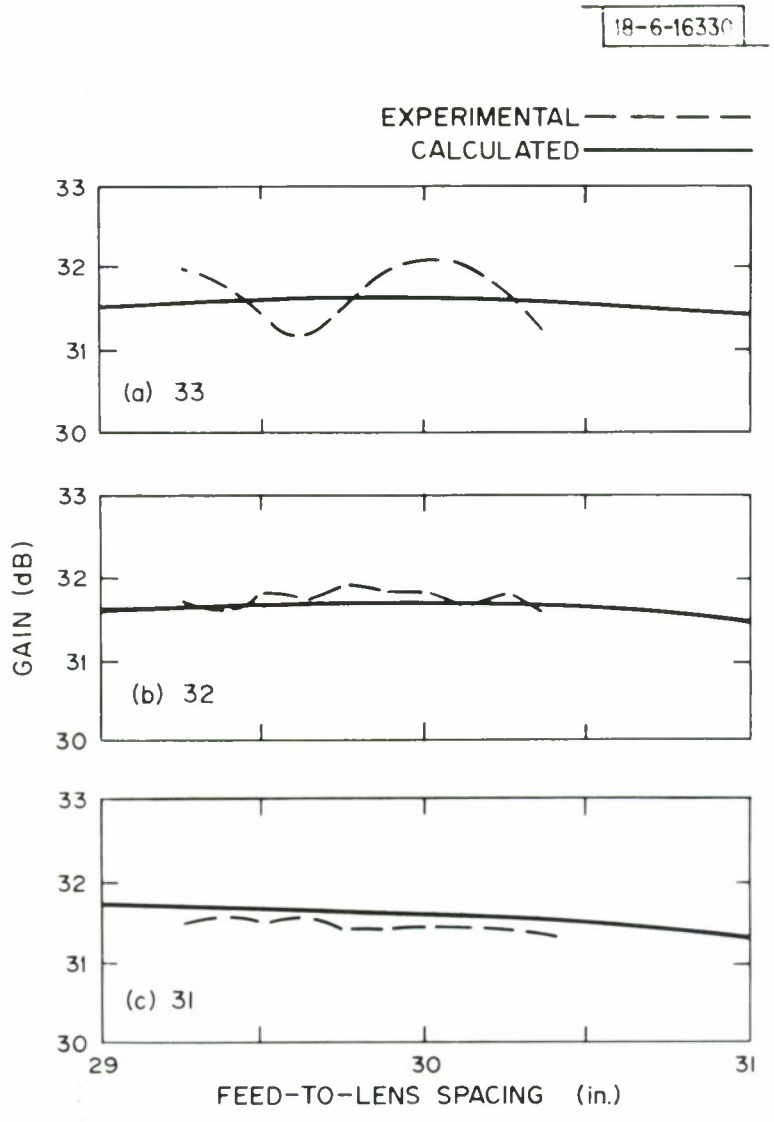

Fig. 22. Gain vs. feed-to-lens spacing for feed No. 33, 32 and 31 and f = 7.680 GHz.

to be used to determine radiation patterns and directivity in lieu of measured data. It follows that the calculated directive gain is also very accurate. However it is necessary to carry the comparison one step further and determine the accuracy of the calculated earth-coverage patterns with prescribed minima.

Sufficient radiation patterns were measured to obtain contour plots corresponding to those shown in Figs. 15-18. (For example,the areas over which a $\geq$ 15-dB reduction in directive gain is obtained by turning off feed horns No. 21, 22, 31 and 32 one at a time are shown in Fig. 23.) The agreement of this data with the calculated data is very good considering the fact that the amplitude and phase uniformity obtained with the 1-to-19 power divider at the input ports of the feed horns were $\pm$ 1 dB and $\pm$ 15 degrees, respectively. The solid curves define the corresponding areas obtained from Fig. 16. Clearly the calculated data is sufficiently accurate to justify its use in the evaluation of any similar lens antenna.

2. Beam-Forming Network

The beam-forming network is without question the "heart" of any multiple-beam antenna system. Multiple beams can be generated by several antenna configurations but the beam-forming network determines the antenna's true flexibility and efficiency. Some recent accomplishments in the art of building ferrite latching phase shifters have rendered the beam-forming network, described in an earlier section of this note, perhaps the most efficient and flexible device of its kind.

In particular, the non-reciprocal latching ferrite phase shifter devel-

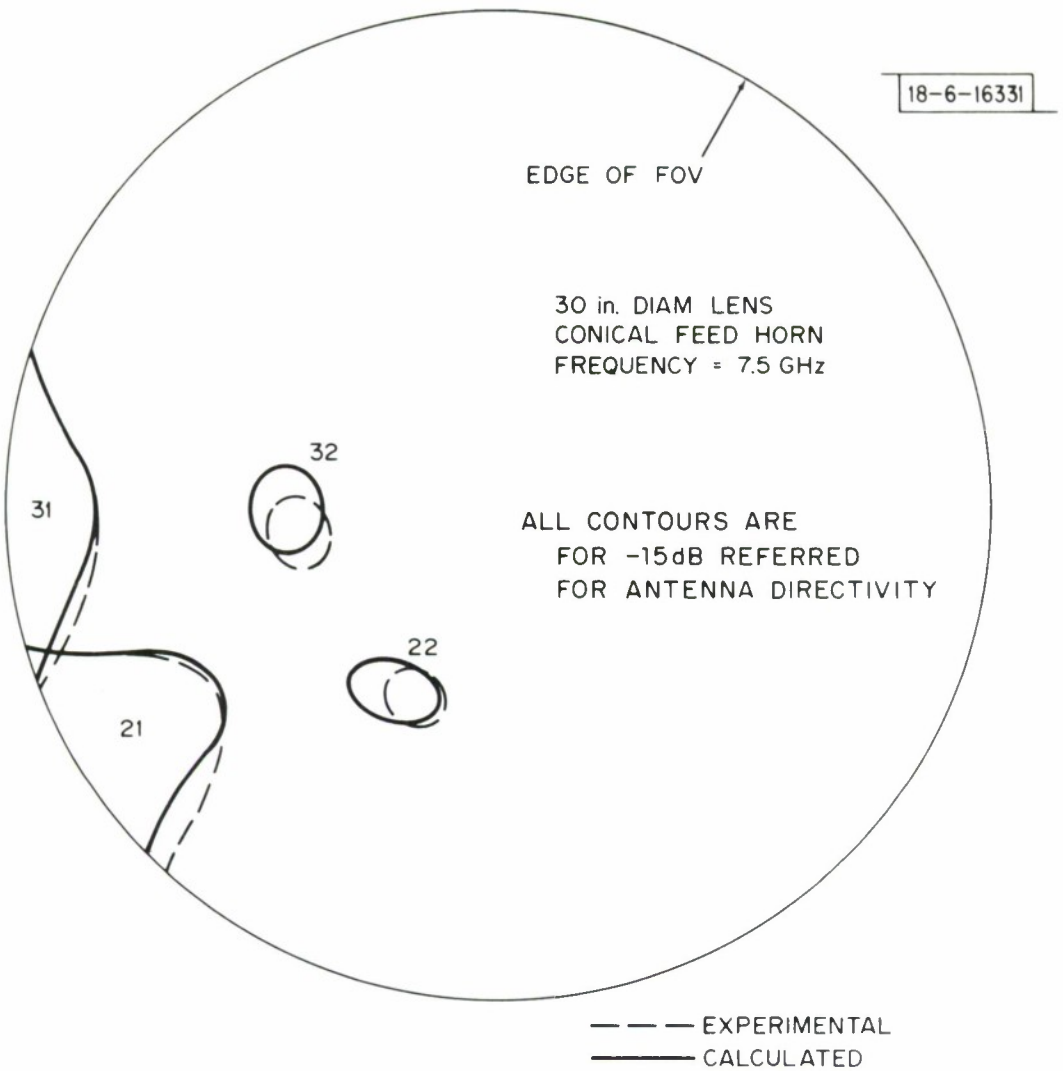

Fig. 23. Contour plot of earth-coverage with a single beam deleted, comparison of experiment and theory.

oped for this program* has an insertion loss of 0.2 ± 0.05 dB over the frequency band 7.25-7.75 GHz. It can change its insertion phase in less than 10 μs. with < 100 microjoules of energy. When a pair are assembled with a matching magic tee and 3-dB short-slot coupler, the assembly, including the ferrite coildrivers, weighs ≈ 15 oz. and has the overall dimensions and configuration shown in Figs. 24 and 25. A beam-forming network for the 19-feed horn array requires 18 variable power dividers (VPD's) identical to those shown in Fig. 24 connected as indicated in Fig. 2. Conceivably the entire BFN could be enclosed in a volume ≈ 0.5 cubic feet, it would weigh ≈ 18 lbs. and the minimum insertion loss between the input port and one of the output ports would be ≈ 1.25 dB. In this section we will briefly describe such a BFN, discuss some measured performance data and use this data to predict some of the expected performance characteristics.

The measured insertion phase of a typical ferrite phase shifter is shown in Fig. 6 as a function of the set pulse width. The device is operated by first driving the ferrite toroid into saturation by applying a 5-μsec or longer pulse with a 5-volt amplitude to the reset control winding. The desired flux density in the toroid, and hence the desired insertion phase, is obtained by applying a 5- volt pulse of the appropriate length (Fig. 6) to the set control winding.† Thus the total operation requires less than

---

*Built by Electromagnetic Sciences, Inc., Atlanta, Georgia.

†For convenience in the design of the drive circuitry, the latching phase shifters have been built with a pair of control windings; one is used for reset and the other for set pulses.

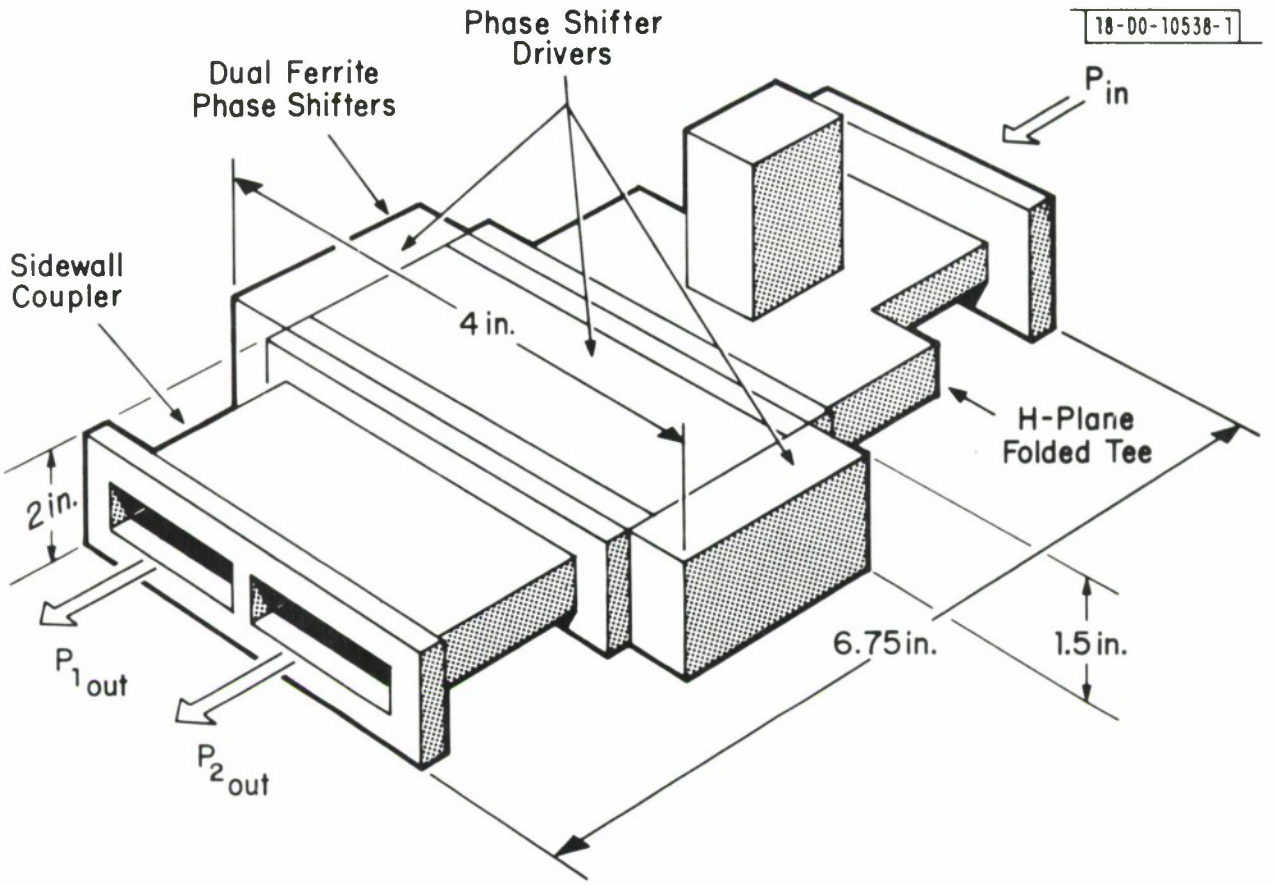

Fig. 24. Variable power divider configuration.

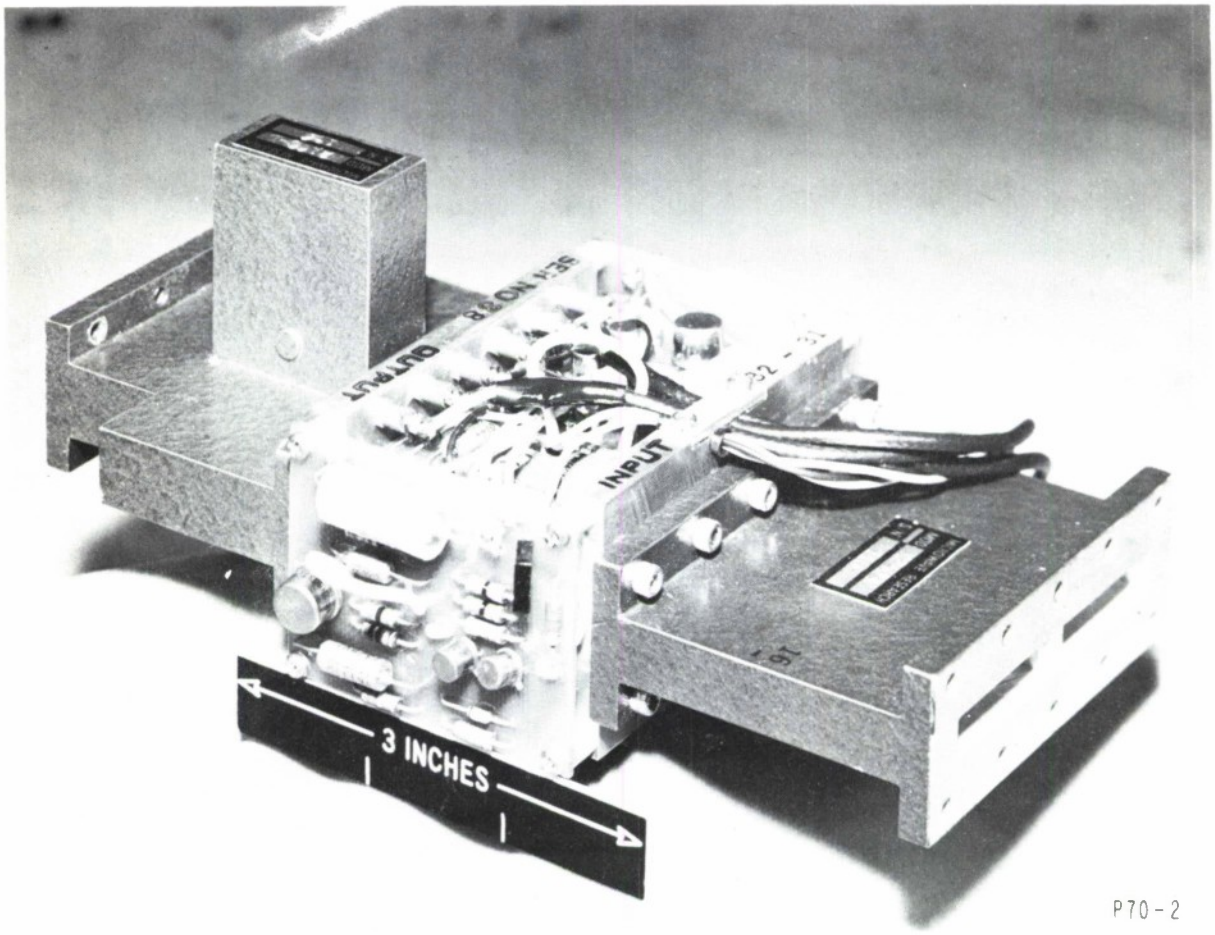

Fig. 25. Experimental variable power divider.

10 μsec. Each VPD utilizes a pair of phase shifters and it is the difference in phase between the two that determines the power division. A change in temperature may change the calibration curve, Fig. 6, of phase shift vs pulse width. If the pair of phase shifters in the VPD are set for equal power split, or approximately equal power split, the change in temperature will have little effect, certainly less than a 1-dB change, for it is likely that both phase shifters will change temperature together and thus change phase together since they are mounted in a common dual-waveguide housing. The most critical effect of temperature occurs when one beam is to be turned off, i.e., a difference of 90° is required between the phase shifters. Preliminary measurements indicate that the variation from the desired 90° is $\approx \pm 5°$ over a temperature range -20°C to +40°C. If this were the only source of phase error, it would result in an "off" beam being > 25 dB down at the temperature extreme rather than turned all the way off. In addition, if the temperature on one pair of phase shifters (i.e., one VPD) is, in general, different than another in the BFN the resulting total insertion phase to any beam port may vary, however, the distribution of power to the beam ports will not be affected. The phase variation may have a small but tolerable effect on the radiation pattern.

It is also true that when forming narrow beams on an earth-coverage pattern an increase in the insertion loss of the beam-forming network might be caused by an incorrect setting of the phase shifters. An examination of Fig. 7, indicates that when the VPD is operated to couple most of its power to a single port, the actual power delivered to that port is not critically

dependent on the set pulse width. Consequently, changes in temperature should not have a profound effect on the performance of the BFN when the antenna is operated in this mode.

When the BFN is operated to produce a minimum in an earth-coverage pattern, at least one VPD will be set to provide the largest possible insertion loss between its input port and one of its output ports. Since our present analysis discussed 15 dB reduction in directive gain and possibly no more than 20 dB reduction could be expected by anything other than a closed loop circuit, one can again examine Fig. 7 and obtain a "feel" for the required accuracy of phase shift when the antenna is operated in the ECPMIN mode. Specifically the pulse could be within $\pm$ 0.2 μsec of the optimum width and still produce an insertion loss in excess of 20 dB. Future investigation will determine whether or not this requirement is compatible with the temperature characteristics of the phase shifters.

In addition to the temperature sensitivity of the ferrite phase shifters, they are a potential source of noise in the form of intermodulation signals. That is, signals, at two or more frequencies, incident on any non-linear device will generate spurious signals at frequencies different from that of the incident signals.

For example, if the incident signals are at frequencies f_1 and f_2 the nonlinear process will generate signals at $f_1 \pm f_2$, $2f_1 \pm f_2$, $2f_2 \pm f_1$, etc., where the order of the intermodulation signal is given by the sum of the coefficients of f_1 and f_2. It can be shown that for the case of a transmit frequency band 7.25 - 7.75 GHz and a receive band 7.9 - 8.4 GHz only odd-

order intermodulation signals are of interest. In particular the third-order IM signal, if it exists, would be of the most interest since in general it will be higher than the fifth, seventh, etc. The amplitude of these signals depends on the nonlinearity of the device, or phenomenon. A section of standard rectangular waveguide produces negligible IM "noise" (the IM signal can be considered noise when it is undesired and appears in the receive frequency band). However, the flange connection can be a significant source of IM noise if it is rough, dirty, distorted, not sufficiently tight, etc. Since the ferrite phase shifter is a "nonlinear" device, it is quite natural to suspect that it is capable of producing a significant level of IM noise. Because of this apparent deficiency, the experimental test setup shown in Fig. 26 was used to determine the probable IM noise-generating characteristics of a ferrite phase shifter used in the BFN.

The output signals of two 15-watt transmitters, one at f_1 = 7.25 GHz and one at f_2 = 7.625 GHz, with appropriate isolation filters and monitors were combined in the output ports of a 3-dB coupler. A load was attached to one port and a bandpass filter was attached to the other to attenuate signals at frequencies outside the range f_1 to f_2. In particular, considerable attenuation was provided to signals 8 GHz and higher; since the third-order IM signal, $2f_2-f_1$ = 8 GHz, was of prime interest. Therefore at the output port of this filter there were two 7.5-watt signals, one at f_1 and one at f_2. The diplexer (consisting of two 3-dB couplers and a pair of matched bandpass (at 8 GHz) filters) served to provide a matched load for signals at f_1 and f_2 and a sensitive detector for signals at 8 Ghz. With the diplexer connected

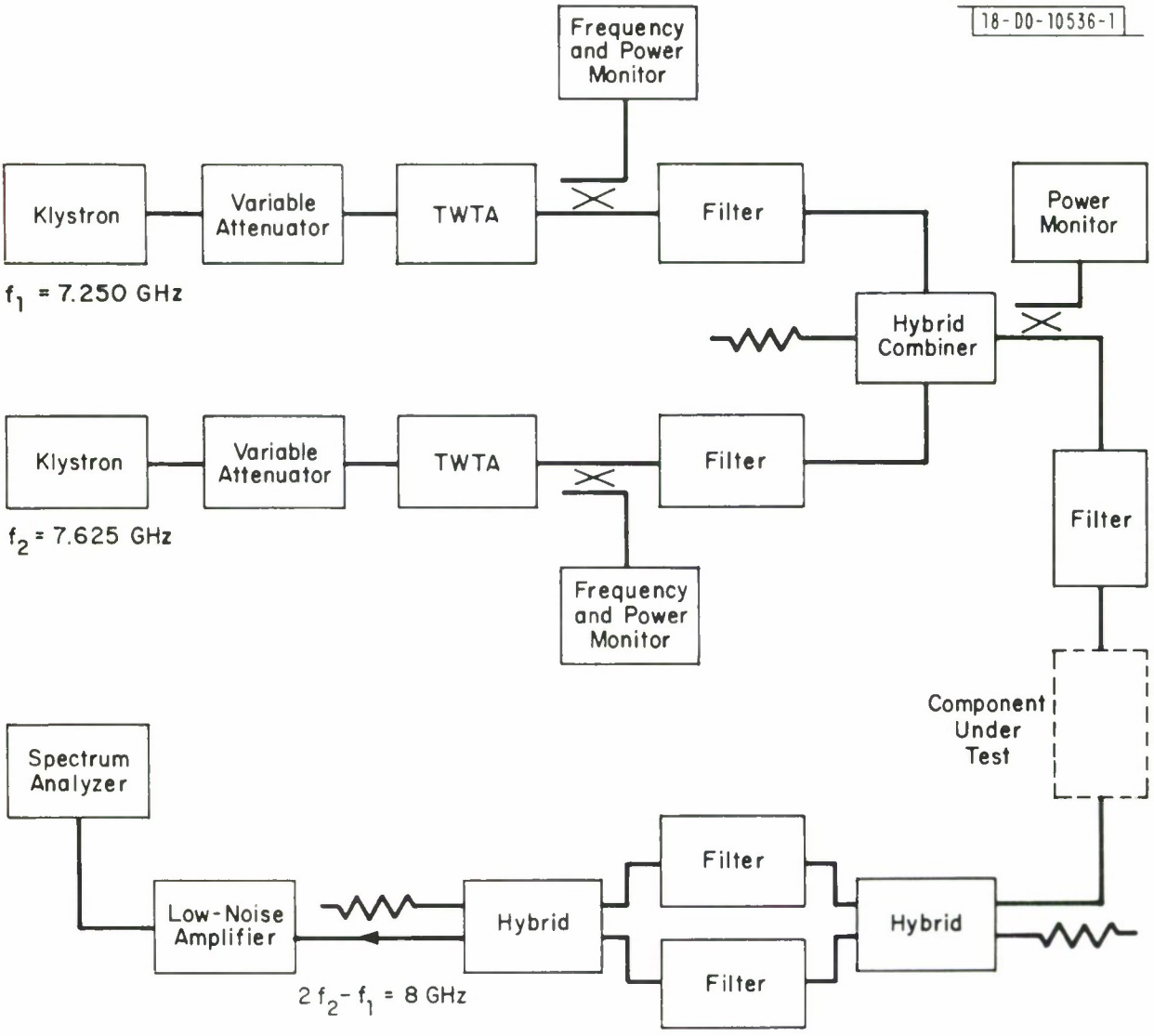

Fig. 26. Intermodulation measurement setup.

directly to the output of the bandpass filter (i.e., component under test is a section of standard waveguide), the IM signal level at 8 GHz was less than -130 dBm. With the ferrite phase shifter introduced in the circuit the IM noise level was as indicated in Fig. 27. The plot of IM noise level as a function of input signal power level demonstrates a 3-dB/dB slope, characteristic of a third-order IM product. This curve also allows one to estimate, for example, that a -87-dBm IM signal at 8 GHz will result if the input sig- power is 20 watts at 7.25 GHz and at 7.625 GHz. This is an interesting result since a proposed frequency plan for the DSCS III satellite and probable use of a 40w and 10w transmitter by the same BFN might give rise to the IM signals under discussion. Since one input signal will be 6 dB less than the other, the IM signal level could be either 6 or 12 dB less than the -87-dBm figure given above. There are two phase shifters in each VPD and as many as five VPD's (see Fig. 2) between the transmitter and the antenna, consequently the IM signal level could be increased 10 dB if we assume noise-like addition. Thus the BFN would produce an IM level between -83 dBm and -89 dBm if the ferrite devices are the predominant IM noise generators. Taking into account an additional attenuation of 70 dB* because separate transmit and receive antennas will be used reduces the expected third-order IM noise expected at the receive frequency to be less than -153 dBm. This certainly appears to be negligible; if it were not, additional filtering in the output ports of the BFN could be used to achieve additional attenuation of the IM-generated signals in the receiver frequency band.

*Measured on DSCS II by TRW.

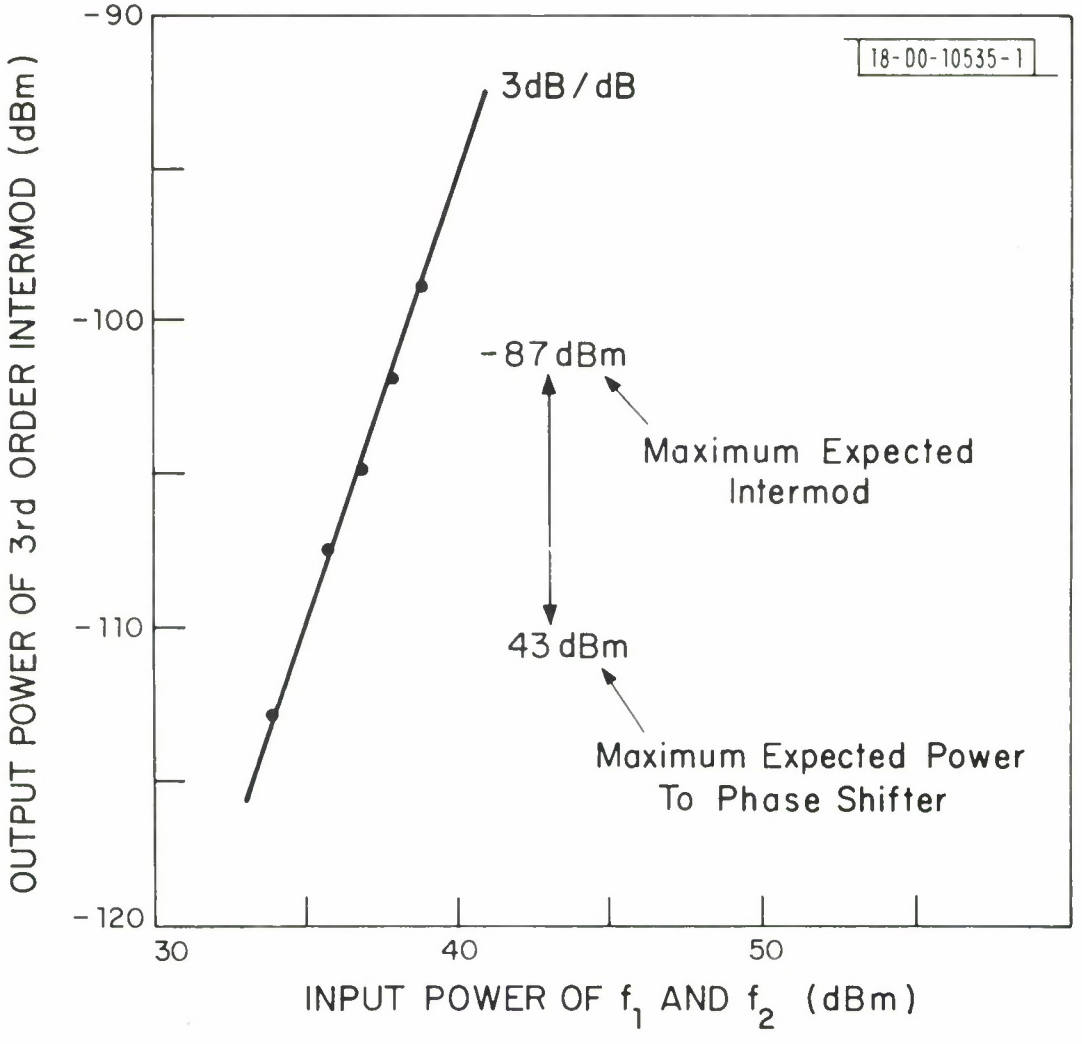

Fig. 27. Input power vs 3rd order intermod for ferrite phase shifter.

If only the fifth and higher order IM signals are present in the receive frequency band, the IM noise level will be in general lower than the -83 dBm level stated above. In fact, the measured fifth-order IM signal level = - 113 dBm with the same setup shown in Fig. 26 and 7.5 watts input power at f_1 and f_2. Extrapolating this result, two 20-watt signals input to a single phase shifter will produce a -93-dBm fifth-order IM signal. The corresponding 10-and 40-W signals into a single VPD will produce an IM signal between -105 dBm and -111 dBm. Thus the BFN would give rise to a fifth-order IM signal $\leq$ - 98 dBm if the ferrite phase shifters are the predominant source of IM signal generation.

Reference

1. A. R. Dion and L. J. Ricardi, "A Variable-Coverage Satellite Antenna System," Proc. IEEE 59, 252 (1971), DDC AD-728190.

REPORT DOCUMENTATION PAGE

READ INSTRUCTIONS BEFORE COMPLETING FORM

1. REPORT NUMBER: ESD-TR-75-110	2. GOVT ACCESSION NO.
3. RECIPIENT'S CATALOG NUMBER	
4. TITLE *(and Subtitle)*: Some Characteristics of a Communication Satellite Multiple-Beam Antenna	5. TYPE OF REPORT & PERIOD COVERED: Technical Note
	6. PERFORMING ORG. REPORT NUMBER: Technical Note 1975-3
7. AUTHOR*(s)*: Ricardi, Leon J.; Dion, Andre R.; Potts, Bing M.; Simmons, Alan J.; DeSize, Lorne K.	8. CONTRACT OR GRANT NUMBER*(s)*: F19628-73-C-0002
9. PERFORMING ORGANIZATION NAME AND ADDRESS: Lincoln Laboratory, M.I.T., P.O. Box 73, Lexington, MA 02173	10. PROGRAM ELEMENT, PROJECT, TASK AREA & WORK UNIT NUMBERS: Element No. 30100
11. CONTROLLING OFFICE NAME AND ADDRESS: Defense Communications Agency, 8th Street & So. Courthouse Road, Arlington, VA 22204	12. REPORT DATE: 28 January 1975
	13. NUMBER OF PAGES: 62
14. MONITORING AGENCY NAME & ADDRESS *(if different from Controlling Office)*: Electronic Systems Division, Hanscom AFB, Bedford, MA 01731	15. SECURITY CLASS. *(of this report)*: Unclassified
	15a. DECLASSIFICATION DOWNGRADING SCHEDULE

16. DISTRIBUTION STATEMENT *(of this Report)*

Approved for public release; distribution unlimited.

17. DISTRIBUTION STATEMENT *(of the abstract entered in Block 20, if different from Report)*

18. SUPPLEMENTARY NOTES

None

19. KEY WORDS *(Continue on reverse side if necessary and identify by block number)*

communication satellite
multiple-beam antenna
radiation patterns
beam-forming network

20. ABSTRACT *(Continue on reverse side if necessary and identify by block number)*

This note describes a waveguide lens antenna system excited by a variable beam-forming network capable of producing a wide range of radiation patterns. These patterns vary from a narrow high-gain beam, equivalent to that of a steerable paraboloid, to the earth-coverage pattern of a wide-coverage communication satellite.